

**A Model for the Lateral Organization of Protein
Molecules in Lipid Bilayers**

Thesis by

Laurence Timothy Pearson

In Partial Fulfillment of the Requirements
for the Degree of
Doctor of Philosophy

California Institute of Technology
Pasadena, California

1984

(Submitted April 30, 1984)

ACKNOWLEDGEMENTS

I have had interactions with many people at Caltech, so much so that it is possible to mention only a few individuals here. I hope those others with whom I have had discussions or collaborated in some way will forgive me their omission.

I have benefited from direct collaboration with Drs. Bob Birge and Phoebe Dea, and from interactions with Drs. Ron Pace and Joe Schuh in the early part of my graduate career.

The most pleasant aspect of my stay in Sunney's group has been my friendship with Utpal Banerjee and Raphael Zidovedski. They are both people for whom I have the deepest respect and admiration and they have my best wishes for the future.

My scientific life at Caltech has been dominated by three men to whom I am extremely grateful.

Jean-Paul Revel has given me free and friendly advice always, and allowed me free use of the facilities in his laboratory for preparation of samples for electron microscopy and for computation using his graphics terminal. My thanks also to Mr. Pat Koen and Mrs. Jean Edens for their assistance.

John Hopfield was always available for discussions during a period of great uncertainty for me. It was an honor to share the science I was trying to do with him.

It took Sunney Chan and me a long time to get to know and trust each

TABLE OF CONTENTS

other. I have come to respect him a great deal both as a scientist and as a human being. His guidance and patience with me as his graduate student ultimately made the difference for me between success and failure in my career here. Sunney was Master of Student Houses for most of my tenure as a resident associate at Caltech. I learned much from him which I will keep with me for the rest of my life. xi

I am proud to have been a resident associate of Ricketts House for three years. I met some remarkable people, grew up myself (more quickly than I might have wanted to in many ways) and had some great times. I made friendships that will last a long time.

Finally, I would like to express my gratitude to Mr. Tsutomu Ohshima and my fellow karateka in the Caltech Karate Club and Shotokan Karate of America for teaching me to express through karate a philosophy of life that has been developing in me for the last ten years. 12

I gratefully acknowledge financial support from Sunney Chan and from the Institute via graduate teaching assistantships. 13

CHAPTER 4 Measurement and Interpretation of Pain

TABLE OF CONTENTS

	<u>Page</u>
ACKNOWLEDGEMENTS	ii
TABLE OF CONTENTS	iv
LIST OF ILLUSTRATIONS AND FIGURES	vi
LIST OF TABLES	xi
A Note on Numbering	xii
ABSTRACT	xiii
CHAPTER 1: Introduction: Protein-Lipid Interactions and Membrane Organization	1
References	12
CHAPTER 2: The Freeze-Fracture Process	13
Introduction	14
The Freezing Process	22
Replication and Observation	27
References	32
CHAPTER 3: Measurement and Interpretation of Pair Distribution Functions from Freeze- Fracture Micrographs	33
Introduction	34
Materials and Methods	37
Results	40
Discussion	52
References	57
CHAPTER 4: A Model for Lipid-Mediated Inter-Protein Interaction in Bilayer Membranes	59
Introduction	60

TABLE OF CONTENTS (continued)

	<u>Page</u>
Theory	61
Pair Distribution Functions	81
Discussion	85
References	94
CHAPTER 5: A Study of the Organizaton of Cytochrome c Oxidase in Lipid Bilayers	97
Introduction	98
Materials and Methods	101
Results	102
Discussion	116
References	130
CHAPTER 6: Summary and Conclusions	132
References	142

LIST OF ILLUSTRATIONS AND FIGURES

	<u>Page</u>
CHAPTER 1	
Figure 1. The Singer Nicholson model of a biological membrane. Protein molecules float at various depths in a "sea" of fluid lipid.	3
Figure 2. Deformation of a bilayer membrane by an intercalated protein molecule. In this case the bilayer is shown as being thinner than the protein. The solubilization energy of the system consists of one term due to direct lipid-protein interaction and one term due to deformation of the bilayer.	6
Figure 3. Some ways in which a bilayer might be postulated to deform to fit a protein molecule.	8
CHAPTER 2	
Figure 1. Freeze fracturing and etching of a lipid bilayer membrane. The bilayer, held in a frozen water matrix, fractures along the plane at its center. The exposed surfaces, which represent the hydrophobic interior of the bilayer, are replicated by platinum.	15
Figure 2. a) Freeze-fracture micrograph of an aqueous suspension of dioleoylphosphatidyl choline frozen from above the phase transition temperature of the lipid. Magnification c. 100000x. b) Freeze-fracture micrograph of a single walled vesicle.	17
Figure 3. a) Diagrammatic representation of a fracture plane of a protein + lipid bilayer recombinant. b) Freeze-fracture micrograph of a bacteriorhodopsin/phosphatidyl choline recombinant. Magnification c. 100000x.	20
Figure 4. a) Configuration of copper discs used for holding an aqueous sample ready for freezing. b) Comparison of two methods of freezing -- propane jet and freon.	24
Figure 5. a) Configuration of the filament and platinum/carbon rod in a platinum gun of the kind commonly used in freeze etch devices. The filament is heated for 7-12	

LIST OF ILLUSTRATIONS AND FIGURES (continued)

	<u>Page</u>
seconds at 2000 V, and 50-80 mA. b) Construction of the platinum/carbon tip. c) The platinum carbon beam is directed onto the exposed surface that is to be replicated.	28
Figure 6. Cross section of the carbon gun. 12-20 V is applied at 20-50 A across the junction between two carbon rods. The point of one rod is held against the surface of another by springs. Carbon is sprayed normal to the surface after the surface has been replicated with the platinum/carbon arrangement shown in figure 5.	30
CHAPTER 3	
Figure 1. Representative micrographs of BR-PC recombinants. a) di 12:0 PC. b) di 14:0 PC. c) di 16:0 PC. The bars represent 150 nm.	41
Figure 2. a) Measured function for BR in di 12:0 PC. Number of particles (N). $N = 1022$, $\rho = 0.0054 \text{ nm}^{-2}$. Frozen from 22°C. b) Measured function for BR in di 14:0 PC (DML). $N = 1678$, $\rho = 0.004 \text{ nm}^{-2}$. Frozen from 34°C. c) Measured functions for BR in di 16:0 PC. $N = 1099$ and 524 , $\rho = 0.003$ and 0.0035 nm^{-2} , respectively. Frozen from 50°C.	43
Figure 3. a) Measured function for bleached rhodopsin in di 12:0 PC from figure 1 of Chen and Hubbell (1973). Frozen from 20°C. $N = 1106$, $\rho = 0.0021 \text{ nm}^{-2}$. b) Measured function for bleached rhodopsin in di 18:1 trans PC, figure 5 of Chen and Hubbell. $N = 668$, $\rho = 0.0017 \text{ nm}^{-2}$	46
Figure 4. a) Measured function for dark-adapted rhodopsin in di 10:0 PC. From figure 1 of Chen and Hubbell. Frozen from 20°C. $N = 819$, $\rho = 0.0021 \text{ nm}^{-2}$. b) Measured function for dark-adapted rhodopsin in di 18:1 trans PC. From figure 4 of Chen and Hubbell. Frozen from 37°C. $N = 955$, $\rho = 0.0014 \text{ nm}^{-2}$. c) Measured function for dark-adapted RH in di 18:1 t. From figure 4 of Chen and Hubbell. Frozen from 20°C. $N = 669$, $\rho = 0.0045 \text{ nm}^{-2}$	49

LIST OF ILLUSTRATIONS AND FIGURES (continued)

	<u>Page</u>
CHAPTER 4	
Figure 1. The dependence of the particle self-energy E_1 (expressed in units of $k_1 (\bar{\phi} - \phi_0)^2$) on the reduced particle size $\sigma_0 (\equiv \eta r_0)$	65
Figure 2. In solving equation 4 for the two-particle problem, .. we invoke the circular boundary condition $\phi = \bar{\phi}$ at both particles. The solution given by equations 8 and 9 is therefore inexact. We illustrate here the departure from circular symmetry by comparing $\bar{\phi}$ with the exact $\phi(r_0)$. The dependence of	68
$\frac{\phi(r_0) - \phi_0}{\bar{\phi} - \phi_0}$	
<p>against θ is shown , where r_0 is some point on the boundary of one particle, and θ is defined as in the diagram. The reduced particle size, σ_0 is taken to be 1.0, and σ', the inter particle separation, is 2.0 and 3.0. The circular boundary condition corresponds to</p>	
$\frac{\phi(r_0) - \phi_0}{\bar{\phi} - \phi_0} = 1.0.$	
Figure 3. Calculated two-particle potential energies (expressed in units of E_1) for various particle sizes ($\eta r_0 = 0.2, 0.5, 0.8$ and 1.1).	72
Figure 4. The segment representing the region of integration used in equation 18.	74
Figure 5. Computer-generated representation of the particle distributions in the EM pictures taken from figure 1 of James and Branton (1973).	83

LIST OF ILLUSTRATIONS AND FIGURES (continued)

	<u>Page</u>
Figure 6. Measured (+) and simulated (-) PDF's for the particle distributions in figures 1a-c of James and Branton (1973). $\Delta r = 10$ nm. a) $\rho = 0.0032 \text{ nm}^{-2}$, $r_O = 5.0$; b) $\rho = .0025 \text{ nm}^{-2}$, $r_O = 4.0$ nm; c) $\rho = 0.0025 \text{ nm}^{-2}$, $r_O = 4.0$ nm.	86
CHAPTER 5	
Figure 1. Freeze-fracture micrographs of cytochrome c oxidase particles in lipid bilayer membranes. Buffer in each case except b) was 0.01 tris, pH 7.4. a) In DMPC. b) in DMPC, plus 1 M sodium chloride. c) In cardiolipin. d) In DMPG. The bar on each photograph represents 100 nm.	103
Figure 2. Micrograph of a structure seen commonly in the oxidase/DMPC low-salt sample. Particles are not intercalated into a bilayer and may represent protein in aqueous suspension or protein-lipid complexes into high protein:lipid mole ratio.	108
Figure 3. PDF's of cytochrome c oxidase in lipid bilayer membranes. The number of particles per membrane ranged from 300-500. a) in DMPC, low-salt sample. b) In DMPC, 1 M sodium chloride. c) In cardiolipin. d) In DMPG.	110
Figure 4. A plot of $V(r)/k_1(\phi_O - \bar{\phi})^2$ against the mean inverse correlation length of the bilayer between two particles $\langle \xi \rangle r'^{-1}$. Each line applies to a single inter particle distance r'	119
Figure 5. a) Splay distortion in lipid bilayer structure at a protein-lipid boundary can be propagated into the bulk of the lipid. b) The effect of splay distortions at protein-lipid boundary producing a curl $n \neq 0$ condition as two protein molecules approach. The length of the arrows represents the projection of the lipid orientation vector onto the membrane surface.	126

LIST OF ILLUSTRATIONS AND FIGURES (continued)

Page

CHAPTER 6

- Figure 1. Sketch of the cross section of the cytochrome
c oxidase molecule in the mitochondrion. 136

LIST OF TABLES

	<u>Page</u>
CHAPTER 4	
Table 1. Values of $\eta r'$ below which I^* exceeds 5% of $M(0)$	77
Table 2. Parameters used in simulating particle distribution functions.	88
CHAPTER 5	
Table 1.	115

ABSTRACT

A Note on Numbering

The numbers of figures and equations given in this thesis apply to the chapter in which they appear. Any equation which is referenced outside the chapter in which it appears will have that fact noted in its reference.

ABSTRACT

Interactions between membrane bound proteins are examined using freeze-fracture etch electron microscopy. The pair distribution functions (PDF's) of protein particles in natural and synthetic membrane systems are examined, and compared with PDF's that are calculated from potential energy functions. In particular, PDF's calculated from the hard-disc only interaction between particles serve as a useful reference for determining whether particle interactions are attractive or repulsive. Of particular interest is the possibility that the lipid bilayer membrane mediates protein interactions. A model is presented for a lipid-mediated interaction that predicts that if protein molecules perturb the bilayer membrane away from its equilibrium (protein free) configuration and that if the perturbation is propagated laterally through the membrane over a sufficient distance, then an attractive interaction is the result.

The model is tested on recombinants of cytochrome c oxidase with dimyristoyl phosphatidyl choline and glycerol and with cardiolipin. Each recombinant is frozen from above the phase transition temperature of the lipid, so the membranes are expected to be fluid. Aggregation of protein into patches is seen, but all PDF's are indicative of a long-ranged repulsion. The model must be modified to account for the repulsion, a modification that would explain the observations in the inclusion of a vector membrane order parameter, namely lipid tilt, into the model. Tilt perturbation can be described by using the formalism already developed for describing nematic and smectic liquid crystals. A repulsive interaction between protein

particles that is analogous to that seen between Schlieren textures in liquid crystals can be shown to occur if protein molecules induce tilt deformations in the bilayer around their boundaries.

CHAPTER 1

Introduction: Protein-Lipid Interactions and Membrane Organization

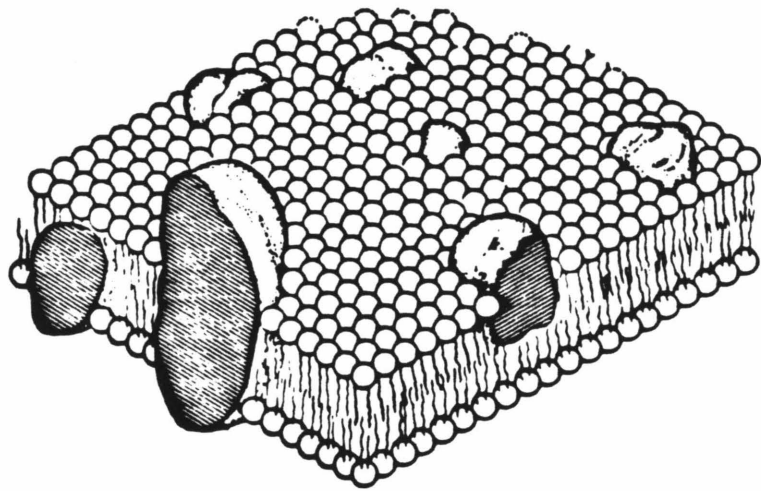
The classical view of biological membrane structure is due to Singer and Nicholson.¹ Figure 1 shows a representation of a membrane from their paper. The dominant lipid structure is a bilayer, into which are inserted protein molecules at various depths. The bilayer has hydrophilic surfaces that bound a hydrophobic interior. An effect known as the "hydrophobic effect"² dictates that a protein molecule should be amphiphilic in order to insert into the membrane thereby matching its hydrophobic and hydrophilic regions with the corresponding regions of the bilayer.

Protein molecules are known to affect the motion and conformation of lipid molecules in bilayers into which they are inserted, and the study of protein-lipid interactions has been a field of intense interest in recent years (see, for example: vol. 37:1-401 of the Biophysical Journal, 1982 for a comprehensive set of papers on protein-lipid interactions). Spectroscopic measurements, sometimes in conjunction with assays of physiological activity or with electron microscopic studies, have been the dominant sources of data in such studies.

Some general patterns from studies of lipids in protein-lipid recombinants can be discerned. For example, most protein molecules appear to immobilize a fraction of spin labeled lipids in protein/lipid/spin labeled lipid recombinants as judged by electron paramagnetic resonance (EPR) spectroscopy.³ Studies using ²H nuclear magnetic resonance (NMR) of deuterated lipids indicate, however, that immobilization is not necessarily occurring on the NMR time scale.^{4,5}

The interpretation of spectroscopic data is aided by considering simple models of how protein molecules may affect neighboring lipids, even if there

Figure 1. The Singer Nicholson model of a biological membrane. Protein molecules float at various depths in a "sea" of fluid lipid.



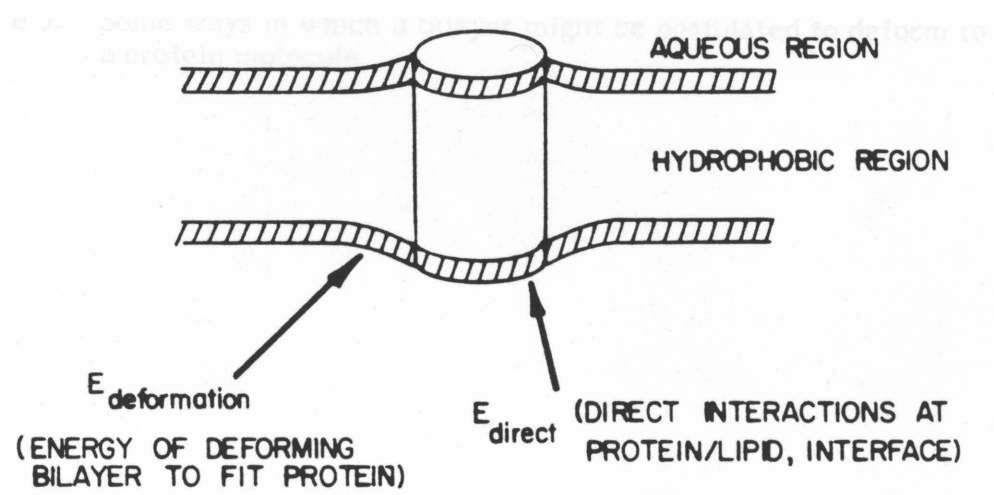
is no strong bonding of lipid to protein. The fact that lipid and protein hydrophilic and hydrophobic surfaces must match means that if there is an intrinsic mismatch between these membrane components -- caused, for example, by differences in width or shape, then either protein or lipid must distort. Distortion of lipid seems the more likely event,⁹ although in some cases protein conformation is known to be influenced by lipid state.¹⁰ The hydrophobic surface that a lipid membrane in its undistorted state presents to a protein is essentially planar, with the plane parallel to the bilayer normal. If a protein molecule has a hydrophobic surface which is (say) conical, then tilt will be induced in lipid molecules adjacent to the protein molecule. Similarly, if a protein hydrophobic surface is parallel to that of the lipids, but of different thickness, then a conformational change will be induced in lipid molecules, a change which is caused by the membrane being required to alter its thickness.

In figure 2 we show diagrammatically a mismatch between protein and the surrounding membrane. There will be an energy of solubilization associated with insertion of the protein into the bilayer, and we have divided this energy into two terms.

$$E_{sol} = E_{direct} + E_{def} \quad (1)$$

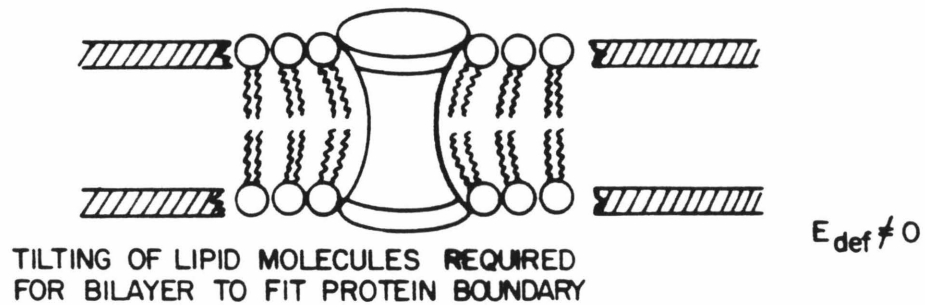
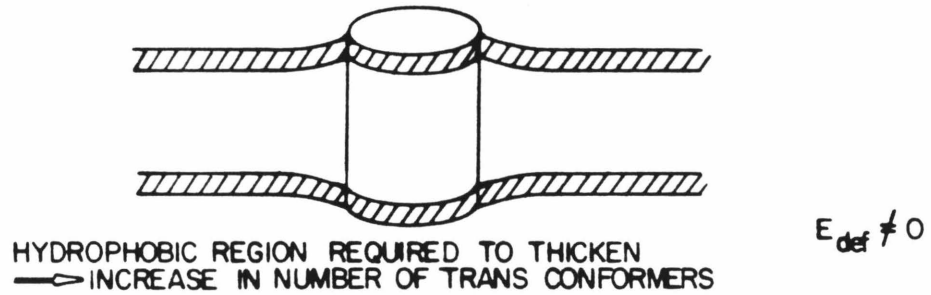
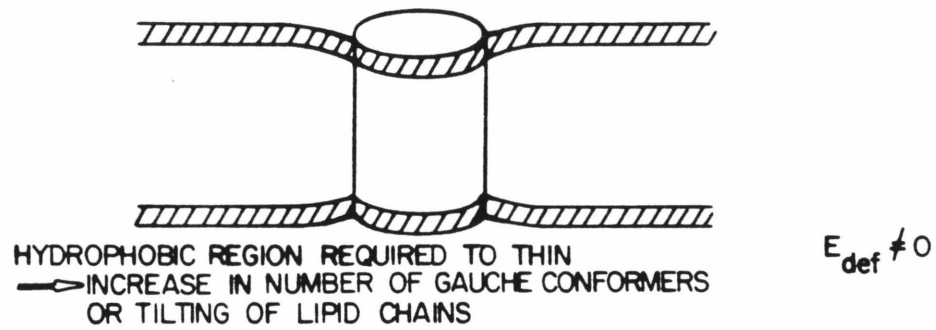
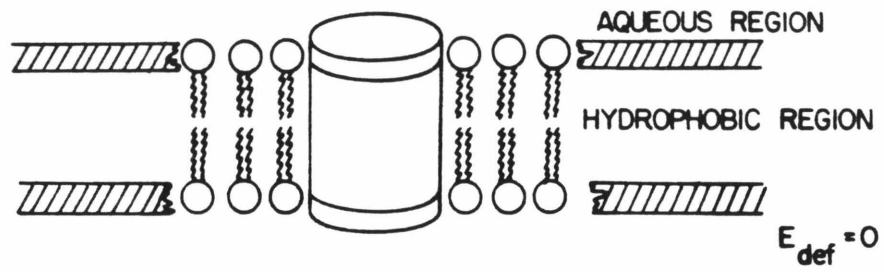
E_{direct} is the direct interaction energy between protein and lipid. E_{def} is a deformation energy that arises because the bilayer has to be deformed away from its equilibrium (protein-free) configuration in order to fit the protein. In figure 3 are shown ways in which the bilayer may have to deform to fit a

Figure 2. Deformation of a bilayer membrane by an intercalated protein molecule. In this case the bilayer is shown as being thinner than the protein. The solubilization energy of the system consists of one term due to direct lipid protein interaction and one term due to deformation of the bilayer.



$$E_{\text{solubilization}} = E_{\text{deformation}} + E_{\text{direct}}$$

Figure 3. Some ways in which a bilayer might be postulated to deform to fit a protein molecule.



protein molecule. Two major types of change in the bilayer may be envisaged. One type of change involves intramolecular conformational changes in the lipid. For example, thickening of the bilayer at some point requires an increase in the number of trans conformers in the lipid hydrocarbon chains that make up the hydrophobic region of the membrane. Another change may take place in which entire lipid molecules may change orientation. For example, a membrane may thin by tilting of the lipid hydrocarbon chains. These effects will be discussed later in this thesis in connection with some experimental results.

A number of theoretical studies have been published that model E_{def} and show that, if protein perturbs lipid, then an inter-protein potential energy is the result.⁶⁻⁸ This lipid mediated inter-protein interaction may be repulsive or attractive depending on the nature of the perturbation of the protein to the lipid.⁸ An inter-protein interaction will be manifested as a change in the distribution of the protein in the membrane. In particular, if protein molecules are confined to the plane of a membrane, then the lateral organization of a protein is a measure of two-dimensional forces between protein molecules. In principle, there is therefore a means other than spectroscopy of lipids to evaluate protein lipid interactions if quantitative access to protein lateral distributions is available.

One experimental technique that provides access to protein lateral distribution is freeze-fracture electron microscopy (FFEM). Using FFEM, membrane bound positions can be visualized directly and measurements made of their lateral positions in a membrane. With judicious choice of experimental conditions and a method for extracting inter particle interactions

from measurements of particle positions, information should be obtainable from freeze-fracture micrographs about protein-protein and protein-lipid interactions.

The object of this thesis is to develop means of quantitating protein interactions by FFEM and to develop models for the lateral organization of proteins using FFEM data as an input. We therefore commence with a discussion of the freeze-fracture process. In subsequent chapters will be shown how measurement of the pair distribution function of protein particles from electron micrographs can be related to the radial correlation function and hence the potential energy function between protein particles. Experiments on protein-lipid recombinants then indicate the conditions necessary for lipid mediated interaction to be manifested in protein lateral distribution.

References and Notes

- (1) S. J. Singer and G. L. Nicholson. Science, **175**, 720-731 (1972).
- (2) C. Tanford. "The Hydrophobic Effect: Formation of Micelles and Biological Membranes"; Wiley: New York, 1980.
- (3) D. Marsh, A. Watts, R. D. Pates, R. Uhl, P. F. Knowles and M. Esmann. Biophys. J., **37**, 265-274 (1982).
- (4) M. R. Paddy, F. W. Dahlquist, J. H. Davis and M. Bloom. Biochemistry, **20**, 3152-3162 (1981).
- (5) S. Y. Kang, H. S. Gutowsky, J. C. Hsung, R. Jacobs, T. E. King, D. Rice and E. Oldfield. Biochemistry , **18**, 3257-3267 (1979).
- (6) S. Marcelja. Biochim. Biophys. Acta, **455**, 1-7 (1976).
- (7) H. Schroder. J. Chem. Phys., **67**, 1617-1619 (1977).
- (8) H. Gruler and E. Sackmann. Croat. Chim. Acta, **49**, 379-388 (1977).
- (9) B. A. Lewis and D. M. Engelman. J. Mol. Biol., **166**, 203-210 (1983).
- (10) P. K. Wolber and B. S. Hudson. Biophys. J., **37**, 253-262 (1982).

CHAPTER 2

The Freeze-Fracture Process

Introduction

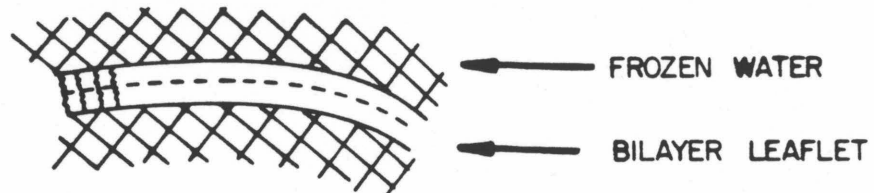
Freeze fracturing is a technique for the preparation of samples prior to observation in transmission electron microscope.¹ As the name suggests, the technique entails freezing a sample, then mechanically fracturing it, thereby exposing two complementary fracture faces (fig. 1). These faces are then given a coating of platinum from an angle to the surface of the face. The coating is sufficiently thick to be seen in the electron microscope and sufficiently thin that structural features of the surface are shadowed by the platinum and thereby appear highlighted against the even platinum background in the microscope.

If the sample contains lipid, then the lipid phases give a clear pattern which is characteristic of the phase in which the lipid exists. For example, consider a pure lipid bilayer in a frozen water matrix undergoing the freeze-fracture process (fig. 1). The sample will fracture along planes of least resistance. In the case of a bilayer this is the center of the bilayer leaflet, where there is no formal chemical bond between the two leaflets. For example, figure 2a shows a micrograph of a sample containing dioleoylphosphatidyl choline (DOPC) multilayers frozen from above T_C of the lipid. Figure 2b shows a single-walled vesicle which has fractured through the middle of the bilayer leaflet.

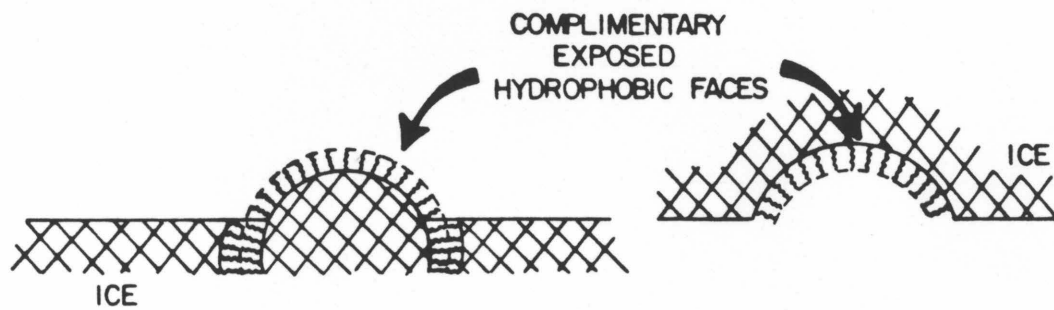
If there is protein inserted into the bilayer (fig. 3a), the fracture pattern now shows particles in the lipid which represent places where the fracture plane encounters a protein molecule or cluster of molecules (fig. 3b). Freeze-fracture electron microscopy can therefore be used to examine the lateral organization of membrane proteins if the freezing process is

Figure 1. Freeze fracturing and etching of a lipid bilayer membrane. The bilayer, held in a frozen water matrix, fractures along the plane at its center. The exposed surfaces, which represent the hydrophobic interior of the bilayer, are replicated by platinum.

FROZEN SPECIMEN



FRACTURED SPECIMEN



ETCHED SPECIMEN

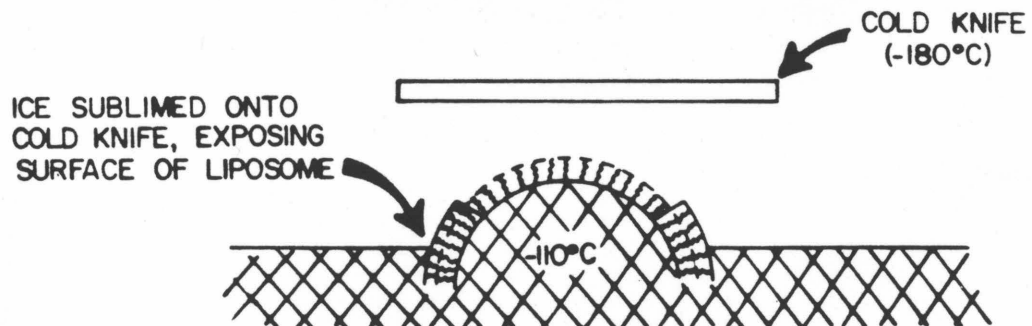
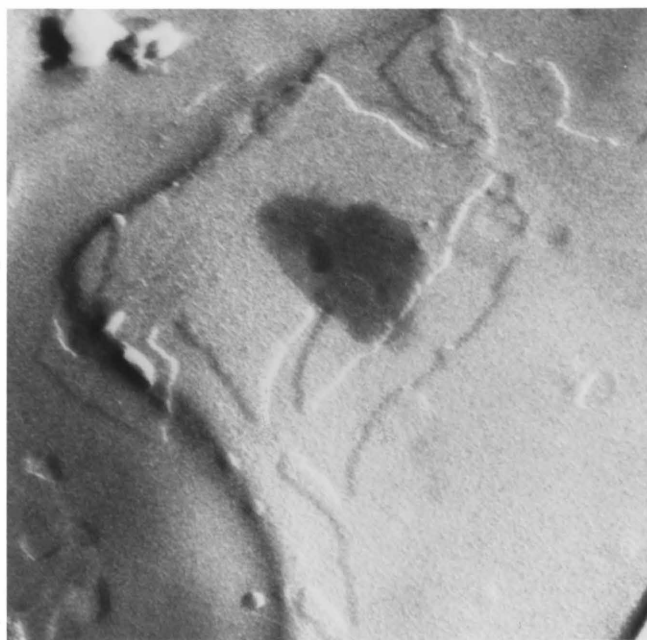


Figure 2. a) Freeze -fracture micrograph of an aqueous suspension of dioleoylphosphatidyl choline frozen from above the phase transition temperature of the lipid. Magnification c. 100000x. b) Freeze fracture micrograph of a single-walled vesicle.

(a)



(b)

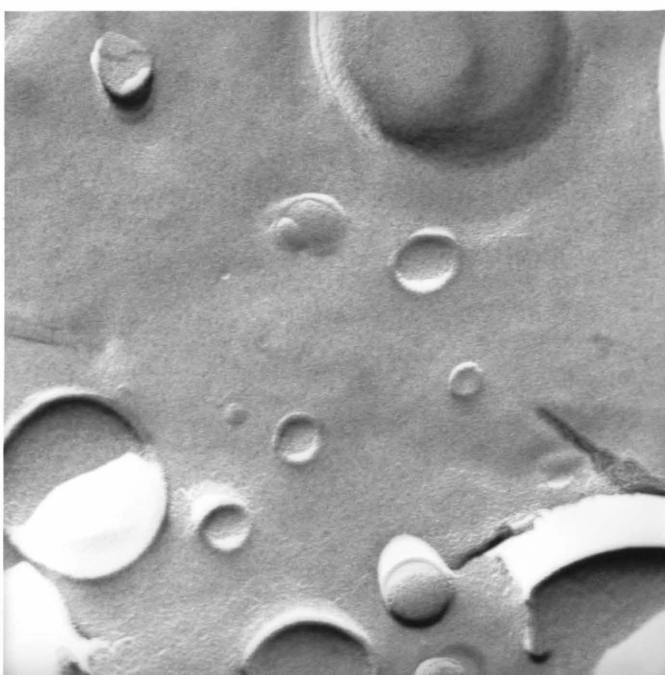
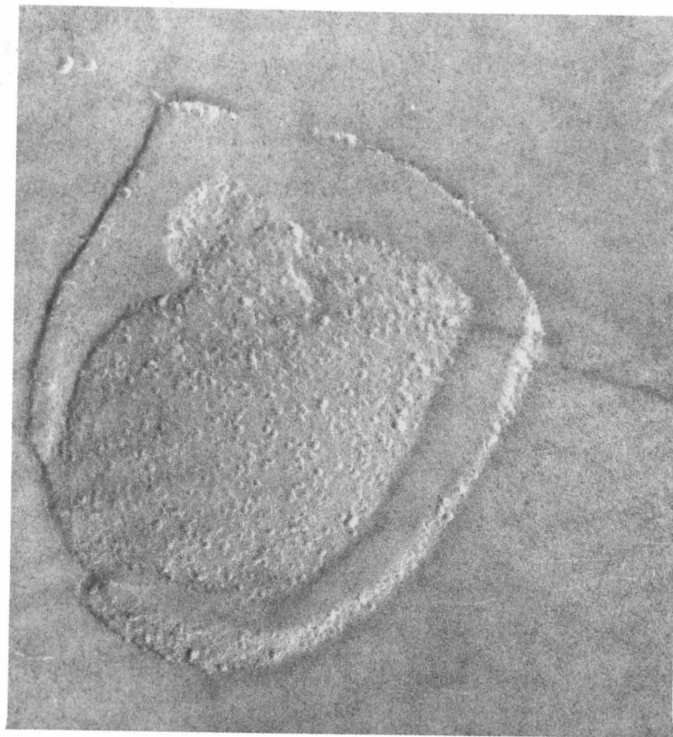


Figure 3. a) Diagrammatic representation of a fracture plane of a protein + lipid bilayer recombinant. b) Freez-fracture micrograph of a bacteriorhodopsin/phosphatidyl choline recombinant. Magnification c. 100000x,

FRACTURE FACE WITH INTERCALATED PROTEIN



sufficiently fast that the structure of the membrane is not disrupted during freezing. We therefore need to examine in more detail the freezing process. In the following sections the freezing and replication process will be described.

The Freezing Process

In using freeze-fracture micrographs for analysis of protein distribution, we assume that the micrograph provides an accurate representation of the protein particle positions in membranes. This can only be the case if the sample, which consists of membrane plus aqueous phase, is frozen sufficiently quickly to prevent significant motion of membrane components relative to each other during freezing. In practice this requires that i) the water in the sample vitrify, as growing ice crystals will alter the membrane morphology, and that ii) lipids are frozen into their gel state with no significant lateral motion of the membrane bound protein. This latter point is particularly significant because protein molecules tend to be aggregated below the phase transition temperature of lipid.

Conventionally, condition i) above is assured by adding 5% glycerol to the sample to inhibit ice formation and ii) is assured by "fixing" the protein positions relative to each other using glycerinaldehyde. In the studies described here, we wish to examine inter-protein interactions in the absence of additives. Micrographs that were taken from the literature for analysis are, unless otherwise stated, obtained from samples without additives. For freeze-fracture work carried out by this author, three fast freezing methods were attempted. The first, due to Bachmann and Schmidt² entailed spraying

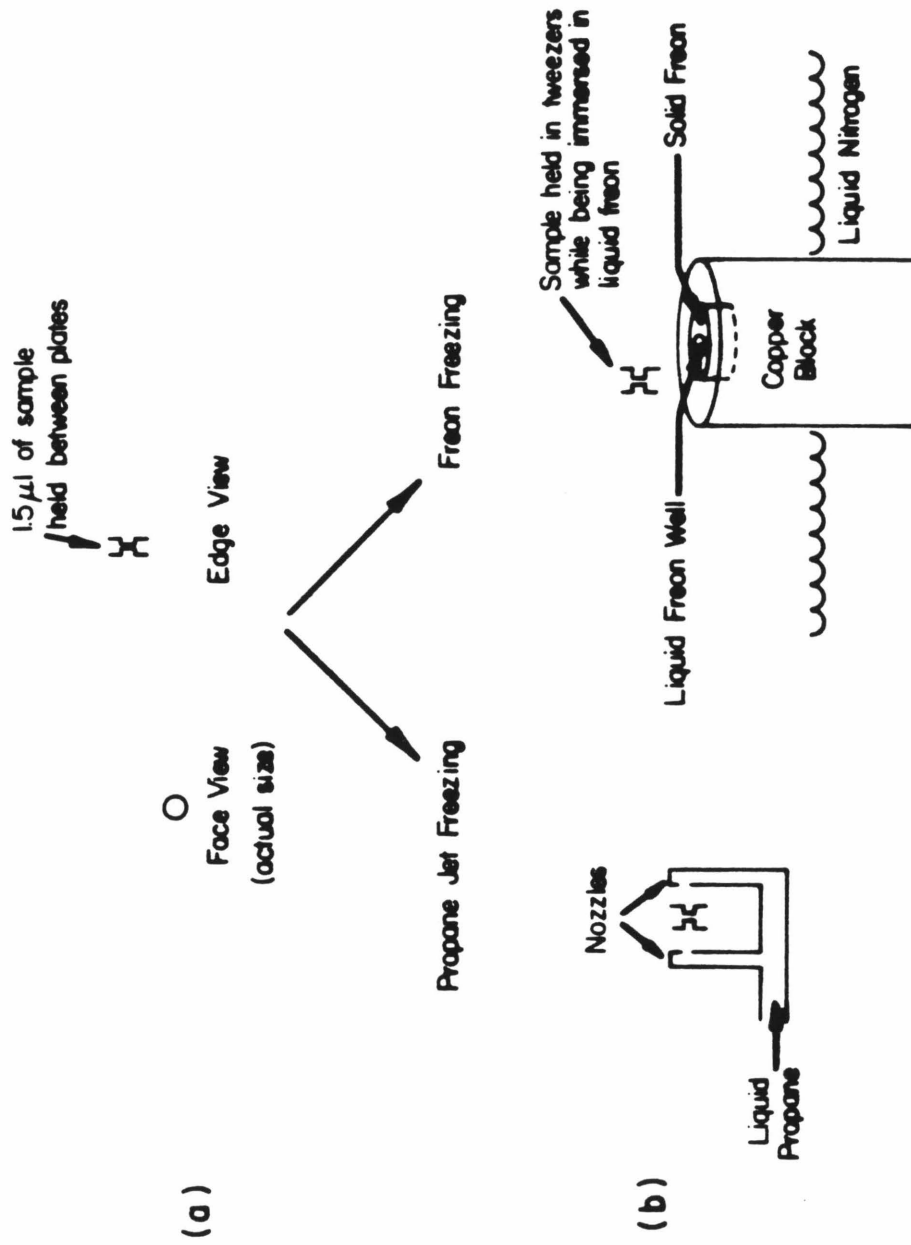
sample through a paint spray gun onto a copper block that was partially immersed in liquid nitrogen. It was found to be impossible to use this method on the fracturing configuration used on the Balzers machine at Caltech. A similar problem was reported by B. Lewis at Yale (private communication).

Alternative methods entailed holding approximately 1.5 μL of sample between two copper discs each 25 μm thick (see fig. 4a) and rapidly freezing the resulting sandwich in either liquid freon 22 or spraying a jet of liquid propane at the sandwich (fig. 4b). The frozen sandwich was then mounted in a Balzers 360M instrument and fractured. The Pt/C replicas obtained were removed from the discs by gently dissolving the discs in approximately 3 M nitric acid. The method using freon 22 was found to be simplest, safest and to give consistently good results both in terms of replica stability and quality of micrograph. Despite the empirical success of the method, it is worthwhile to examine briefly the physics of the freezing process in more detail and establish some idea of why it works.

For the purposes of examining particle positions, the worst possible case occurs if, during the period t ongoing from quenching temperature T to T_C , the protein particles have a lateral diffusion constant equivalent to that which they have at temperature T . Denote the diffusion constant by D . The average distance moved by each particle is then:

$$\begin{aligned} \langle r \rangle_t &= 2\pi \int_0^{\infty} r (4\pi Dt)^{-1} \exp \left(\frac{-r^2}{4Dt} \right) r dr \\ &= 8\sqrt{\pi} (Dt)^{1/2} \end{aligned} \quad (1)$$

Figure 4. a) Configuration of copper discs used for holding an aqueous sample ready for freezing. b) Comparison of two methods of freezing -- propane jet and freon.



For reconstituted membrane bond proteins, D is of the order of $10^{-10} \text{ cm}^2 \text{ sec}^{-1}$. This places a value of $\langle r \rangle$ at $1500 \text{ t}^{1/2} \text{ nm}$. If T is 298 K and T_C is (say) 10 K lower, a freezing rate of 10^6 K sec^{-1} is required to keep $\langle r \rangle < 10 \text{ nm}$. As will be seen from data presented later in this thesis, freezing rates obtained using the processes described above are adequate to prevent partial aggregation's being detected in particle patterns even as judged using quantitative methods for evaluating such patterns.

The rate of formation of ice crystals and their size distribution and also the rate of heat transfer of heat from a sample through copper discs to a cooling medium have been analyzed mathematically by Kopstad and Elgsaeter.^{3,4} Their results may be summarized as follows. Ice crystals grow from nucleation points in a specimen well below the freezing point of the specimen. Solidification of water without significant ice crystal growth will take place only below about 230 K , which we denote as T_v , the vitrification temperature. Actual specimen solidification by ice crystal formation takes place within, at most, 3 K of T_v , and cooling rate must be 10^5 K sec^{-1} in order that ice crystal average size be less than around 10^2 nm (thereby allowing for a significant number of smaller crystals and vitrified water). This constraint on rate of cooling is considerably relaxed in the presence of solute in the aqueous phase.

Theoretical analysis of heat transfer rates through copper discs indicates that using a substantially cooler medium than liquid freon (e.g., liquid propane) does not result in a substantially improved specimen cooling rate. Within $20 \text{ } \mu\text{m}$ of the copper surface, a vitrification rate of up to 10^7 K sec^{-1} can be obtained, which is adequate for rapid freezing of membrane

suspensions. That this is the case is confirmed by studies presented in this thesis. Pt/C replicas were produced which showed neither distortion of membranes by ice crystals nor the kind of aggregation of proteins that is seen in micrographs of lipid-protein recombinants frozen from below the lipid T_C .

Replication and Observation

In this section we briefly summarize the procedures used for replicating the surface that is exposed after fracturing.

A Balzers 360M freeze etch device was used in studies carried out by this author for fracturing and replication. A platinum (Pt) layer of the order of 1 nm thick is required and the platinum beam was obtained from a gun which utilizes an electron beam to vaporize a Pt bead that is held in a carbon (C) rod (fig. 5). The quantity of Pt falling on the sample was monitored using a quartz crystal monitor which was held near the replicated surface. The monitor shut off the Pt gun when enough Pt had been detected. Samples were shadowed from 30° to the horizontal phase.

Carbon coatings were applied to the replicas to give them strength for being handled. The coating is of the order of 200 \AA thick. The gun configuration is shown in figure 5.

Replicas were examined in a Philips 201C transmission electron microscope in the laboratory of Dr. Jean Paul Revel. Operating voltage was 80 kV and photographic images were taken on 35 mm film from which 8" x 10" prints were made. Magnification ranged from 150,000-200,000 on the final print depending on the magnification setting of the microscope.

Figure 5. a) Configuration of the filament and platinum/carbon rod in a platinum gun of the kind commonly used in freeze etch devices. The filament is heated for 7-12 seconds at 2000 V, and 50-80 mA. b) Construction of the platinum/carbon tip. c) The platinum carbon beam is directed onto the exposed surface that is to be replicated.

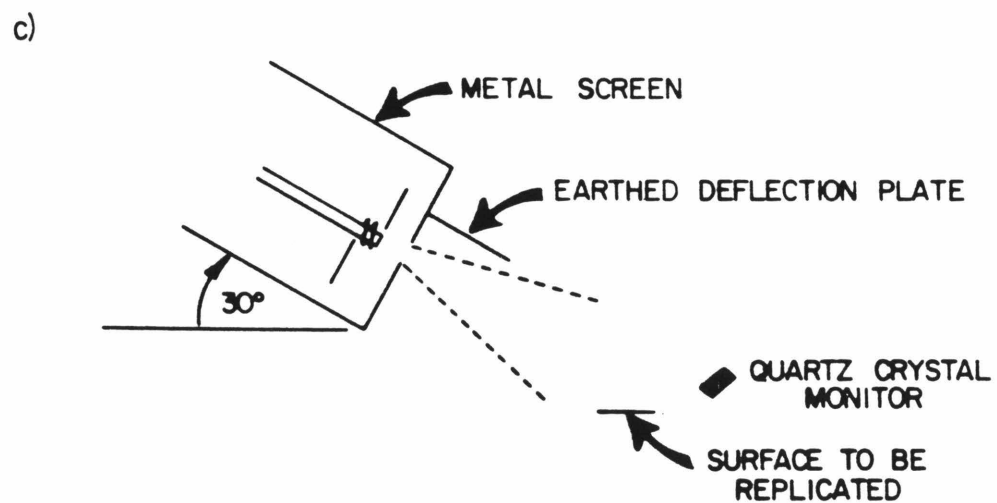
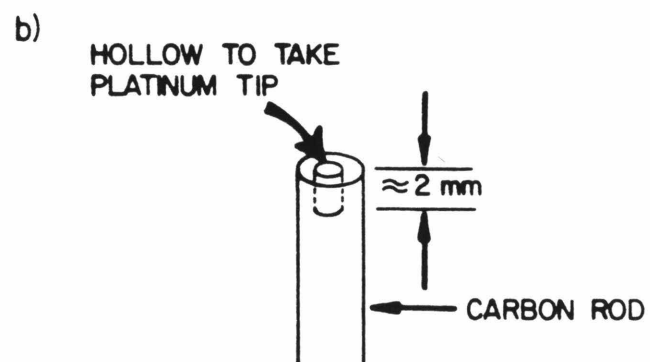
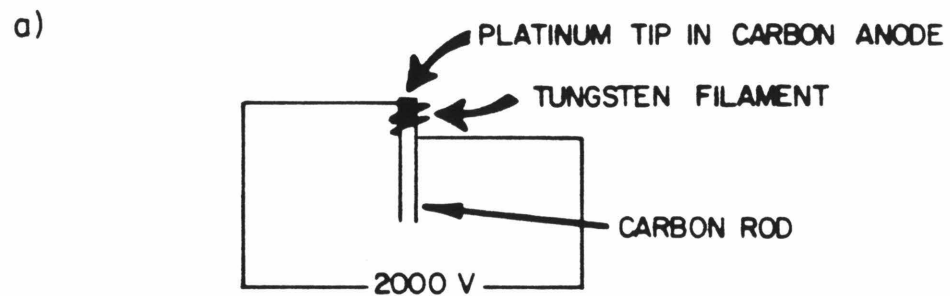
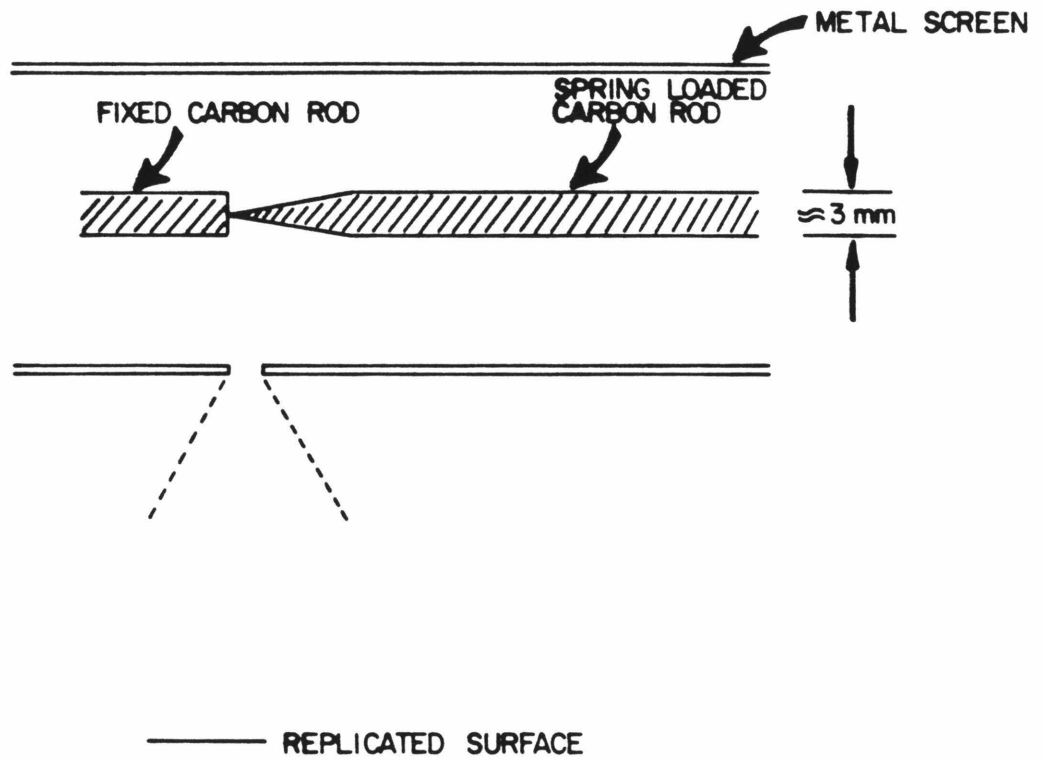


Figure 6. Cross section of the carbon gun. 12-20 V is applied at 20-50 A across the junction between two carbon rods. The point of one rod is held against the surface of another by springs. Carbon is sprayed normal to the surface after the surface has been replicated with the platinum/carbon arrangement shown in figure 5.



References and Notes

- (1) D. Branton. Phil. Trans. Roy Soc., London, **B261**, 133-138 (1971).
- (2) L. Bachmann and W. W. Schmidt. Proc. Natl. Acad. Sci., U.S.A., **68**, 2149-2152 (1971).
- (3) G. Kopstad and A. Elgsaeter. Biophys. J., **40**, 155-162 (1982).
- (4) G. Kopstad and A. Elgsaeter. Biophys. J., **40**, 163-170 (1982).

CHAPTER 3

Measurement and Interpretation of Pair Distribution
Functions from Freeze-Fracture Micrographs

Introduction

The aggregation state of proteins in biological membranes is an important aspect of membrane organization. It has been shown that the lateral organization of membrane bound proteins can change during events of physiological significance.¹⁻⁴ The most direct method for determining the aggregation state of membrane proteins is freeze-fracture electron microscopy, which yields qualitative information upon simple visual inspection. Recently methods have been devised to quantitate the distribution of particles in micrographs, either by digitization of particle coordinates or by using less elaborate counting techniques.^{5,6}

In the present chapter we employ the pair distribution function⁷⁻⁹ to obtain a quantitative measure of the aggregation state of two trans membrane proteins, bacteriorhodopsin (BR) and rhodopsin (RH) in vesicles made with phosphatidyl cholines (PCs) of several acyl chain lengths. From the measured functions one can deduce the strength of protein-protein interactions, even if these interactions are too weak to produce aggregation which is visually obvious. Of particular interest is the possibility of lipid-mediated interactions,^{10,11} a subject on which there are few data at the moment.

Spectroscopic experiments indicate that protein molecules perturb lipid order, and these data have been interpreted in terms of a perturbed boundary around the protein. Although it is possible that the boundary is a single layer of molecules, there is mounting data to suggest that it extends further.¹² In the latter case, there will be characteristic length associated with decay of the lipid state to its bulk configuration, and the perturbation

around the protein-lipid boundary would be expected to decay smoothly into the bulk lipid.

One way in which proteins could affect neighboring lipids is by altering the local membrane thickness. There are two ways that this thickness can be modified. The intramolecular conformational state of the hydrocarbon chains or the head groups can be affected, or tilting of entire lipid molecules may occur. For example, if the thickness of the hydrocarbon region of a membrane is less than that of the hydrophobic region of a protein, in order for the membrane to accommodate the protein, the lipid hydrocarbon chains would need to be in a more extended conformation with a higher proportion of trans isomers per hydrocarbon chain than in the bulk lipid. The situation is somewhat more complex if the membrane hydrophobic region has to contract to accommodate the protein. In this case accommodation could take place either by an increase in the average tilt of the lipid chains with respect to the bilayer axis, or by further disordering of the chains via an increase in the fraction of gauche isomers along the hydrocarbon chain. It is apparent that for there to be a match between bilayer and protein, there will be a boundary region interfacing the protein surface with the bulk lipid.

If the proteins perturb the lipid to any significant extent, over a few nanometers laterally in the membrane, this lipid protein interaction should have observable effects on the protein pair distribution function.¹³ The pair distribution function, $w(r, \Delta r)$ is defined by the ratio of the mean density of particles located in an annulus between r and $r + \Delta r$ from the center of an average particle, to the mean overall density. A more fundamental quantity is the radial correlation function, $g(r)$, which is related to the pair

distribution function by

$$w(r, \Delta r) = \frac{2 \int_r^{r+\Delta r} g(r) r dr}{r(r + 2\Delta r)} \quad (1)$$

Although the pair distribution function, $w(r, \Delta r)$, approaches $g(r)$ as Δr approaches zero, for the relatively small (<1000) number of particles generally seen in freeze-fracture micrographs, only the pair distribution function can be determined reliably (using a finite annulus size in order to minimize relative errors in the determination of the number of particles in the annulus). Despite this shortcoming, the radial correlation function for a set of particles remains useful in that it can be readily calculated from a given inter particle potential energy function between the protein particles.¹⁴

We illustrate this by considering here a number of special situations. If the protein particles were randomly diffusing points of infinitesimal size, it can be shown that $g(r)$, and hence $w(r, \Delta r)$ would be identically 1.0. If the particles were instead hard discs of radius r_0 , then $g(r)$ would assume more of a structure,¹⁴ which at sufficiently high overall particle density would consist of a peak at $r = 2r_0$ corresponding to a first coordination shell, followed by a region of lower density at $r \sim 4r_0$. This pair distribution function can be calculated from the potential energy function

$$\begin{aligned} V(r) &= 0 & r > 2r_0 \\ V(r) &= \infty & r < 2r_0 \end{aligned} \quad (2)$$

The usefulness of this hard-disc model is that deviations of actually observed $g(r)$ or $w(r,\Delta r)$ from this result could be used to indicate additional attractive or repulsive inter particle interactions.

It should be emphasized that implicit in the above relationships is the assumption that the radial correlation function, and hence the inter particle potential energy function, is radially symmetric. If there is an additional angular correlation between particle positions, equation 1 for $w(r,\Delta r)$ must be written in terms of a more general function including angular and radial correlations. We neglect angular correlations in the present treatment but note at this juncture that the magnitude and shape of the pair distribution function $w(r,\Delta r)$ yields information about radial correlations which can be related directly to the form of inter particle interactions.

Materials and Methods

BR-Lipid Recombinant. Micrographs of BR-lipid recombinants were kindly supplied by B. A. Lewis. The preparation of BR-lipid recombinants is described in detail by B. A. Lewis and D. M. Engelman¹⁵ and is summarized below.

BR was separated from its native lipid by the method of Huang et al.¹⁶ All operations were performed in the dark at 0-4°C.

PC's were from Calbiochem and were lyophilized and dissolved in 2% Na cholate buffer (0.01 M tris HCl, 0.15 M NaCl, pH 8) with brief sonication.

To prepare BR-lipid recombinants, the lipid and BR solutions were mixed under dim red light and subsequently dialyzed against 0.01 M tris HCl, 0.15 M NaCl, pH 8 in a foil-covered flask at 4°C. After at least three days

of dialysis, the vesicles were centrifuged at $104,000 \times g$ through continuous sucrose gradients, 10-45% (w/w). All preparations yielded a single band. The vesicle bands were washed two or three times in buffer, 0.01 M Na acetate, pH 5.

For electron microscopy the BR-lipid recombinants were spray-frozen by the method of Bachmann and Schmidt^{6,17} using a Balzers spray-freeze apparatus (Balzers Union, Sagamore, New Hampshire) with a thermally controlled spray gun. Fracturing and replication were performed in a Balzers freeze etch unit, BAF 301, at temperatures of -115 to -135°C and pressures of 1 to 8×10^{-7} torr. Deposition of Pt and C from electron beam electrodes was controlled by a quartz crystal monitor to a thickness of 25 and 100 \AA , respectively. Replicas were examined in a Philips EM 201 at 80 kV and at magnifications of $20,000$ to $40,000\times$. Photographs from the microscope were enlarged to $150,000$ to $200,000\times$ for measurement of pair distribution function.

RH-Lipid Recombinants. EM pictures of dark-adapted and bleached RH were taken from Chen and Hubbell.¹⁸ The pictures used were of samples which had been frozen from above the phase transition temperature of the lipid. For dark-adapted RH the pictures chosen were of those recombinants in di 10:0 PC frozen from 20°C , and di 18:1 trans PC frozen from 37°C and 20°C and for bleached RH-recombinants in di 12:0 PC and di 18:1 trans PC frozen from 20°C .

Protein Distribution Functions. Protein pair distribution functions were determined by measuring particle coordinates from the EM pictures, calculating the inter particle distances and counting the number of

inter particle distances that lie within the annulus r to $r + \Delta r$. Particle coordinates were taken on the Tektronix graphics tablet in Dr. Jean Paul Revel's laboratory at Caltech and processed on the Chemistry Department VAX 11/780 computer.

Measured distribution functions were compensated for picture-edge effects by simulating random distributions in a square of the same area as that of the membrane analyzed. Up to ten simulations were analyzed and the average pair distribution function taken as a baseline for the membrane measurements. Changing the shape of the test area from a square to a rectangle had negligible effect on the baseline. A value of $\Delta r = 10$ nm was used in calculating $w(r, \Delta r)$. This choice produced a reasonably noise-free distribution function while retaining the major details of the first peak in the function. The number of particles (N) in the picture was required to be greater than about 500 to minimize artifacts due to noise.

Theoretical "hard-disc" pair distribution functions were obtained using the potential energy function of equation 2. The correlation function $g(r)$, was calculated using the Percus-Yevick and Ornstein-Zernike equations. The Ornstein-Zernike equation 3 permits us to relate the indirect correlation function $h(r)$ of a system of particles to the direct correlation function $c(r)$.

$$h(r) = g(r) - 1 = c(r) + \rho \int c(|r - s|) h(s) d^2s \quad (3)$$

At the densities used in this study the direct correlation function is well approximated by the Percus-Yevick relation (eq. 4):

$$c(r) = g(r) \{1 - \exp [V(r)/kT]\} . \quad (4)$$

We solved equations 3 and 4 iteratively using the numerical algorithm of Lado.¹⁴

Results

Figure 1 shows micrographs of BR reconstituted into di 12:0 PC, di 14:0 PC and di 16:0 PC. Areas of membrane which showed even shadowing were chosen in order to minimize artifacts due to membrane curvature. There appeared to be no gross protein aggregation due to the freezing process in any of the pictures we examined. Rearrangement of the protein particles, in particular, a tendency to aggregate, should be reflected in the pair distribution function as an apparent attractive interaction between particles.

The most significant characteristics of the measured functions for the purposes of comparison with the calculated functions are the magnitude of the function at the peak and its rate of decay toward the asymptotic value as $r \rightarrow \infty$. Inter particle interaction should be reflected in these features of the pair distribution function. In particular, an attractive interaction between particles would result in the peak's being larger and decaying more slowly than the hard-disc model. For each of the measured functions presented here, we show for comparison (dashed line on the same figure) the corresponding function calculated for the hard-disc model for the corresponding density and particle radius. The error bar shown on each measured function represents $\pm 1/\sqrt{n}$, where n is the number of inter particle distances that were

Figure 1. Representative micrographs of BR-PC recombinants. a) di 12:0 PC. b) di 14:0 PC. c) di 16:0 PC. The bars represent 150 nm.

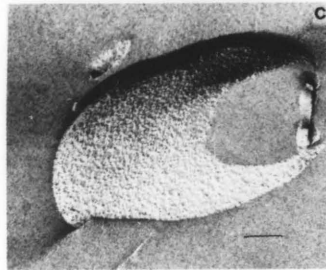
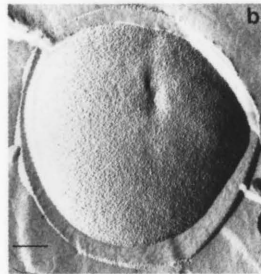
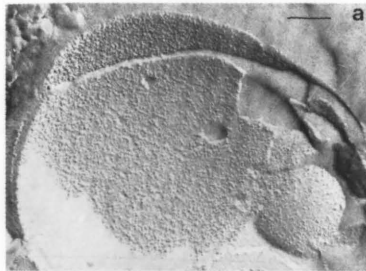
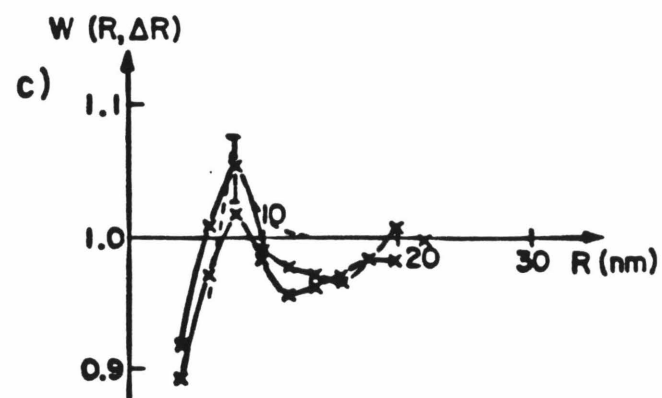
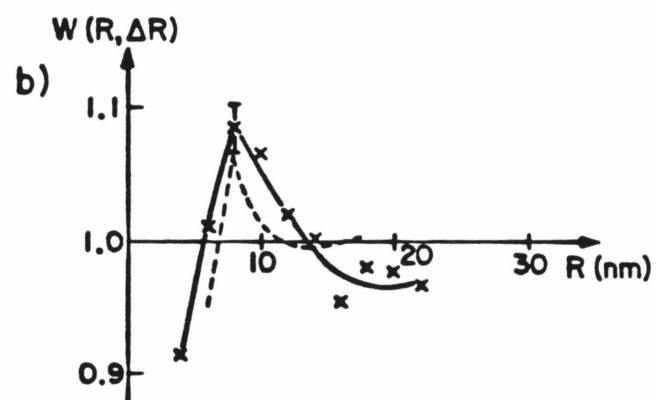
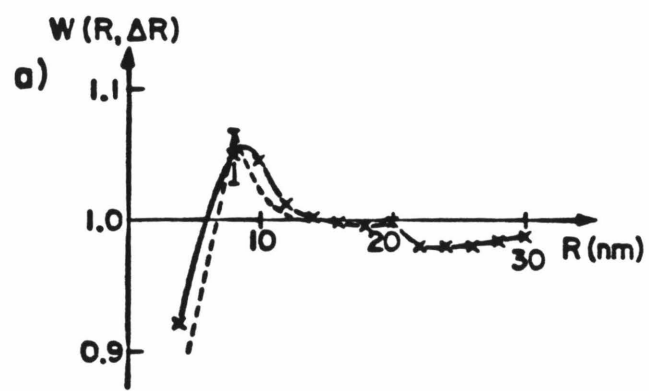


Figure 2. a) Measured function for BR in di 12:0 PC. Number of particles (N). $N = 1022$, $\rho = 0.0054 \text{ nm}^{-2}$. Frozen from 22°C . b) Measured function for BR in di 14:0 PC (DML). $N = 1678$, $\rho = 0.004 \text{ nm}^{-2}$. Frozen from 34°C . c) Measured functions for BR in di 16:0 PC. $N = 1099$ and 524 , $\rho = 0.003$ and 0.0035 nm^{-2} , respectively. Frozen from 50°C .

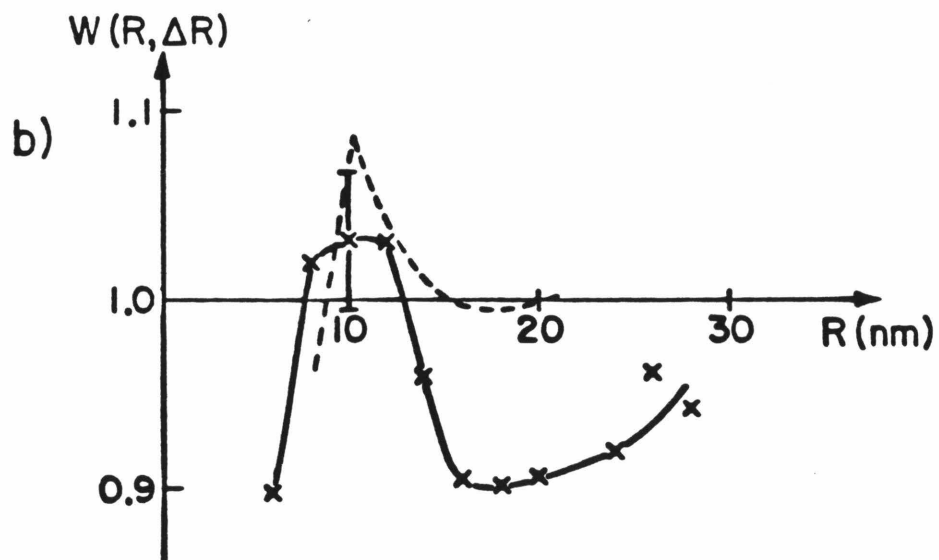
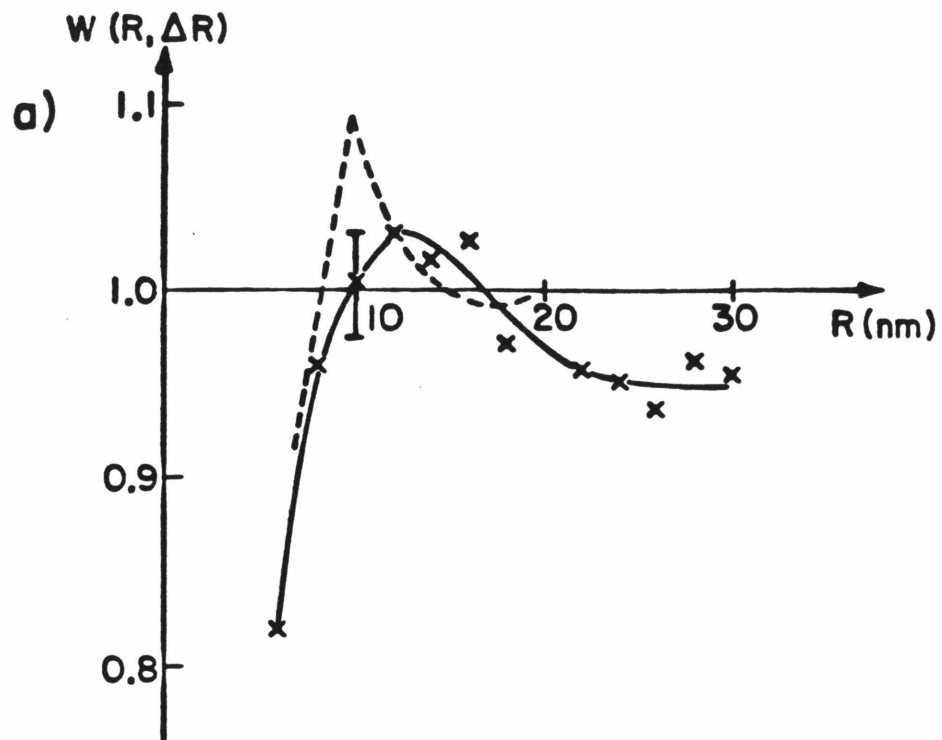


used to calculate the value of that function at $r = 2r_0$. We now consider the results obtained for each protein in turn.

Bacteriorhodopsin. The measured functions are shown in figure 2a-c. Comparison with the calculated function indicates that in all three lipids, the protein is well modeled by the hard-disc interaction. In the di 12:0 and di 14:0 samples the tail of the first peak decays less rapidly than the model function in the region between $r = 8.0$ to 14.0 nm, though even in these cases the magnitude of the peak is consistent with the randomly diffusing hard-disc model. These data support previous conclusions, that the distribution of this protein in the plane of the membrane is random when incorporated into bilayers of hydrophobic region thickness up to 10 \AA less than the protein. The observed random distributions also support the assumption that no significant aggregation of protein particles has occurred during the freezing process.

Bleached Rhodopsin. The measured functions are shown in figure 3a and b. The functions are more difficult to interpret, particularly as they do not seem to decay to 1.0 as r increases beyond the first peak, as in the case of the BR-PC recombinants. This suggests that equation 1 may not be holding exactly for these systems, possibly because the radial correlation function is no longer radially symmetric. This lack of radial symmetry is seen clearly in certain of the rhodopsin pictures where there appear to be patches of lipid ringed by particles. Despite this complication, the difference in magnitude between the first peak and the asymptotic value of $w(r, \Delta r)$ should still be representative of inter particle interactions. In particular, the magnitude of the first peak can still be compared to that of the hard-disc model in order to ascertain whether there are additional

Figure 3. a) Measured function for bleached rhodopsin in di 12:0 PC from figure 1 of Chen and Hubbell (1973). Frozen from 20°C. $N = 1106$, $\rho = 0.0021 \text{ nm}^{-2}$. b) Measured function for bleached rhodopsin in di 18:1 trans PC, figure 5 of Chen and Hubbell. $N = 668$, $\rho = 0.0017 \text{ nm}^{-2}$.



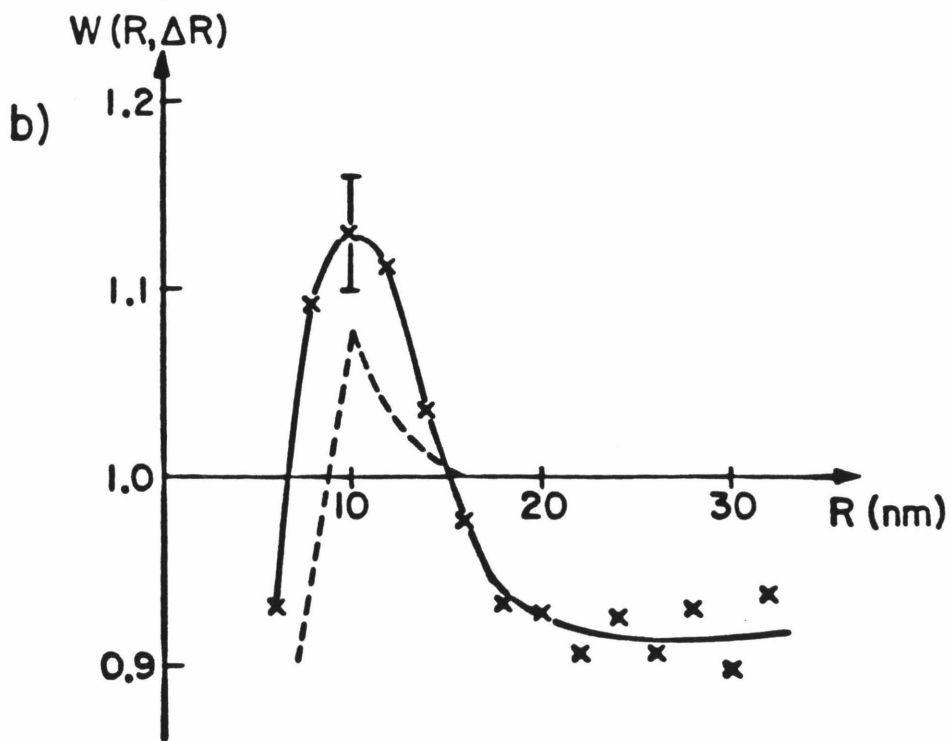
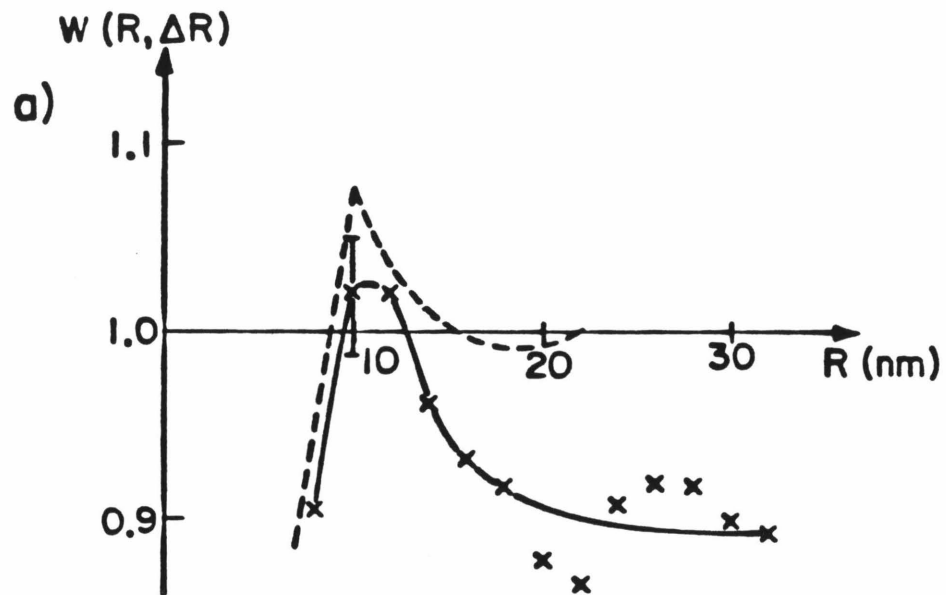
interactions.

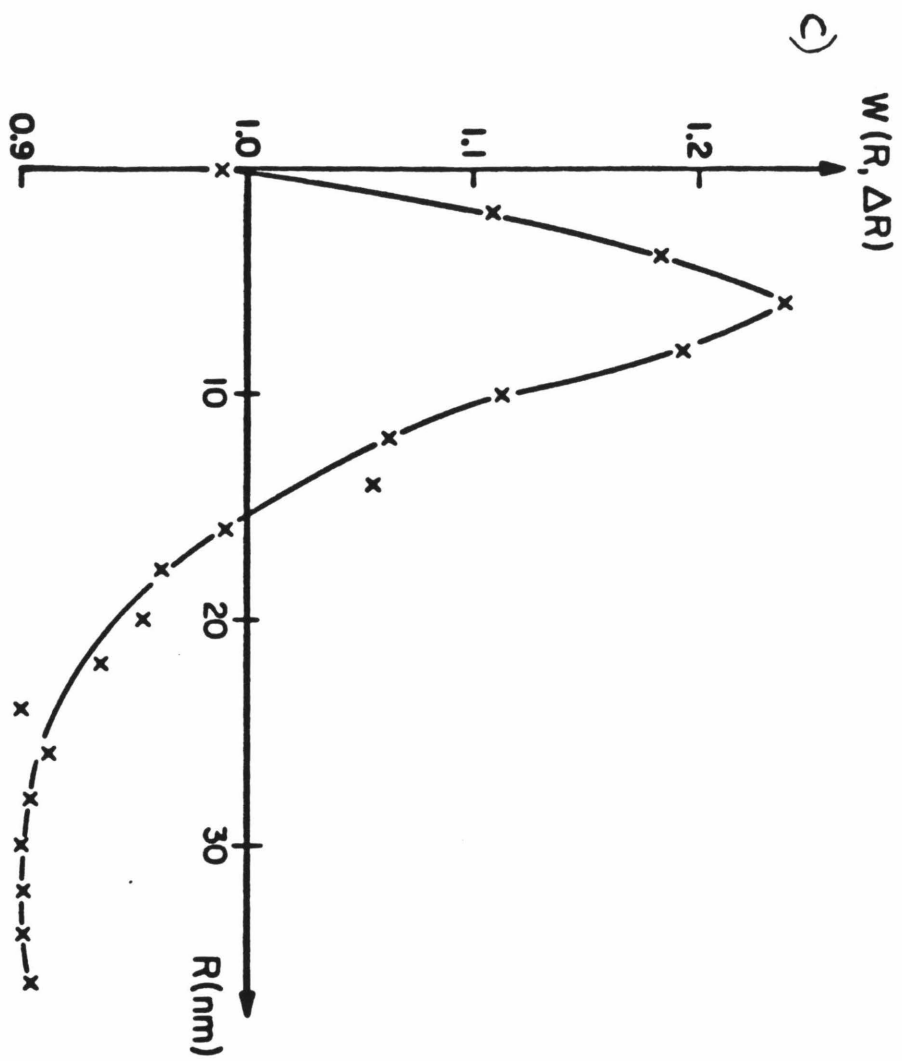
In both di 12:0 PC and di 18:1 trans PC, the size of the first peak in the bleached RH pair distribution functions is less than that of the calculated function using the hard-disc model. In general a value of $g(r)$, and hence $w(r, \Delta r)$, less than that calculated for a system of hard discs suggests that there is a repulsive inter particle interaction that extends beyond particle boundaries tending to keep particles apart.

Dark-Adapted Rhodopsin. The EM picture of dark-adapted rhodopsin in di 18:1 trans PC frozen from 20°C (fig. 4a of Chen and Hubbell) shows the protein to be obviously highly aggregated although the aggregates are dispersed throughout the lipid phase. We chose to examine the picture of the di 18:1 trans-RH sample frozen from 37°C in order to ascertain whether the correlation persists at the higher temperature. Figures 5a and b show the measured pair distribution functions deduced from the data of Chen and Hubbell for dark-adapted rhodopsin -- di 10:0 PC and di 18:1 trans PC recombinants frozen from 20°C and 37°C, respectively.

The magnitude of the peak in the pair distribution function obtained from the 10:0 RH recombinant is consistent with the functions measured from the bleached RH pictures. In the di 18:1 trans PC-RH sample frozen from 37°C, however, the peak is significantly larger and the rate of decay of the function from its peak is slower than the random hard-disc mode. These features of the pair distribution function suggest that in dark-adapted RH-di 18:1 recombinants there is an attractive interaction between protein particles. Since this interaction does not exist in the thinner bilayer, it is therefore probably lipid-mediated. These observations lend credence to ideas

Figure 4. a) Measured function for dark-adapted rhodopsin in di 10:0 PC. From figure 1 of Chen and Hubbell. Frozen from 20°C. $N = 819$, $\rho = 0.0021 \text{ nm}$. b) Measured function for dark-adapted rhodopsin in di 18:1 trans PC. From figure 4 of Chen and Hubbell. Frozen from 37°C. $N = 955$, $\rho = 0.0014 \text{ nm}^{-2}$. c) Measured function for dark-adapted RH in di 18:1 t. From figure 4 of Chen and Hubbell. Frozen from 20°C. $N = 669$, $\rho = 0.0045 \text{ nm}^{-2}$.





of lipid-mediated interactions proposed previously.^{11,13}

In figure 5c we show for comparison the pair distribution function deduced from the EM picture of dark-adapted RH in di 18:1 frozen from 20°C reported by Chen and Hubbell. Here the protein is visibly aggregated. Aggregation is manifested as a relatively large value at the peak in $w(r, \Delta r)$. In addition, the peak occurs at a lower value of r than in the other measured functions for RH-PC systems. This appears to be a general effect which we have noted in all measurements taken from pictures of partially aggregated systems.

Discussion

We have examined in this study the pair distribution functions of BR, bleached RH and dark-adapted RH in PC bilayers.

There appears to be negligible difference between the measured functions for the BR-PC systems and those calculated from a model in which the only interaction is a hard repulsive core. The value of $2r_0$ measured from the positions of the peaks in the PDF's is ~ 8 nm, which is in accordance with the diameter of the particles seen in the freeze-fracture micrographs. Although this figure is approximately twice that deduced by Peters and Cherry¹⁹ from measurements of the lateral diffusion coefficient of the protein in di 14:0 PC, it is consistent with the size of the BR trimer,²⁰ the state of aggregation often implicated for this protein. It is also likely that a freeze-fracture particle of BR represents a protein molecule with one or two boundary layers of lipid relatively tightly bound.

The bleached RH di 12:0 PC and di 18:1 trans PC and dark-adapted RH

of di 10:0 PC systems show deviations from the hard-disc model which may be due to longer range inter particle repulsions. For dark-adapted rhodopsin-di 18:1 trans PC recombinants, however, the results are strikingly different. The freeze-fracture micrograph from Chen and Hubbell¹⁸ of a sample frozen from 20°C shows visible aggregation. We have shown that even at 37°C, where the aggregation is not readily apparent from the EM picture, the protein distribution is not equivalent to that in which there is only a hard repulsive core interaction between molecules, but that there appears to be an additional attractive component in the interaction.

These results can be understood in terms of the probable behavior of the lipids at the protein-lipid boundary and their effect or lack of effect on subsequent lipid solvation layers. When a protein is reconstituted into a bilayer for which the equilibrium thickness of the hydrophobic region does not match that of the protein, there are two possible consequences. The molecules may remain undeformed, thereby exposing the protein hydrophobic region to the aqueous phase in the case where the protein is thicker than the bilayer, or exposing the hydrophilic region of the protein to the hydrocarbon region of the bilayer if the protein is thinner. Alternatively, the bilayers or the proteins may deform at some energetic cost²¹ to match their respective hydrophobic regions. Estimates of the energy cost of exposure of the protein hydrophobic surface to water suggest that if insufficient deformation occurs to match the hydrophobic regions, aggregation of the protein molecules will take place. Such aggregation has been observed in BR di 10:0 PC recombinants.¹⁵ In this case the acyl chains, even if fully extended are probably too short to match the hydrophobic surface of the protein.

Deformation of the bilayer or protein is the more likely event when its energy cost is lower than the corresponding cost due to loss of entropy upon aggregation. The results of Parsegian et al.²¹ suggest that deformation of the bilayer is energetically inexpensive, less than 1 kT for a 20% change in membrane surface area. The presence of a single phase in all the recombinant systems studied here shows that either the proteins are changing conformation to accommodate the bilayer, or the bilayer deforms to fit the protein. The latter possibility seems more likely in view of the relatively large conformational changes that would have to take place for a protein to accommodate a wide range of bilayer thicknesses.

If there is a deformation to the bilayer and it is propagated over a significant characteristic length in the membrane, an intermolecular potential energy will result,¹³ which would be seen in the measured pair distribution functions. This is not seen in any of the systems studied here in which the membrane is thinner than the protein. An interaction is seen, however, in dark-adapted RH-di 18:1 trans PC recombinants, in which the membranes are significantly thicker than those of other lipids used although not, it should be noted, particularly thick relative to most natural bilayer membranes.

In order to postulate an explanation for this effect we consider the cases of thick and thin membranes in turn. Consider first the case where the bilayer is thinner than the protein. If the bilayer deforms to fit the protein, stretching of the hydrocarbon region of the bilayer must occur at the protein-lipid boundary. Our results suggest, that in the system we study here, the intermolecular conformational change that leads to this stretching is not

propagated to any extent laterally through the membrane.

The observation of an interaction in dark-adapted RH-di 18:1 trans PC recombinants suggests that the nature of the effect that this protein has on di 18:1 trans PC bilayers is fundamentally different from that in the other systems examined. If the hydrophobic region of the bilayer formed by di 18:1 PC were thicker than that of the dark-adapted RH molecule, then the lipid molecules could tilt at the protein-lipid boundary, or there could be a conformational change in the lipid head group or hydrocarbon chain region. In any case, the change in the bilayer structure must be propagated over a significant distance in the membrane for an inter-protein interaction to result. This change could involve tilting of the lipid molecules which may possibly be propagated through the bilayer by low-frequency cooperative motions of the hydrocarbon chains, or propagation of the direct lipid-protein interaction may be via the hydrophilic or interface regions of the lipid, or merely increased disorder of the lipid-hydrocarbon chains. Further studies are needed to characterize the altered bilayer conformation.

The different behavior noted here between bleached and dark-adapted RH in di 18:1 trans PC deserves comment. It is possible that the hydrophobic surface of rhodopsin thickens on bleaching so that the bleached molecule is no longer thinner than the di 18:1 trans bilayer. Such a conformational change could reduce the perturbation of the bilayer by the protein and thus reduce the lipid-mediated inter-protein attraction. This suggests the possibility of a role for lipid-protein interactions in the physiological function of RH which should be investigated further.²² However, other explanations for the dramatic difference in aggregation of the two states of RH cannot be

ruled out without further data. For instance, bleaching of RH might increase the net molecular charge, leading to an intermolecular repulsive interaction which could counteract lipid-mediated or other attraction. The fact that bleached RH remains unaggregated below the lipid-phase transition temperature in all lipids examined, under conditions in which dark-adapted RH aggregates, is more consistent with the latter explanation. Again, more experiments are required to establish the nature of the difference between dark-adapted and bleached RH in di 18:1 trans bilayers.

There are other factors that may affect the observed protein distribution of the RH-lipid recombinants which are difficult to exclude completely at this time. First, pictures of the RH-PC recombinants were of multilamellar dispersions. It is possible that interbilayer interactions may affect lateral proteins. Similarly, in a multilamellar protein-lipid recombinant, the orientation of the protein incorporated into the recombinant membranes may influence the lateral distribution of membrane-bound proteins. Unfortunately, we have not data at this point which allow us to assess the importance of this question in the present situation. Finally, the different distribution seen in various RH-di 18:1 trans recombinants might originate from protein denaturation in the dark-adapted RH recombinants. This seems rather unlikely, as the aggregation seems to be lipid-specific, with the extent of aggregation seemingly only a function of temperature from which the sample was frozen. We await future work to clarify some of these points.

References and Notes

- (1) R. S. Decker and D. S. Friend. J. Cell Biol., **62**, 32-47 (1974).
- (2) D. S. Friend and I. Rudolf. J. Cell Biol., **63**, 466-479 (1974).
- (3) L. A. Staehelin. J. Cell Biol., **71**, 136-158 (1976).
- (4) R. S. Weinstein. Cancer Res., **36**, 2518-2524 (1976).
- (5) J. T. Donnell and L. X. Finegold. Biophys. J., **35**, 783-798 (1981).
- (6) R.P. Pearson, S. W. Hui and T. P. Stewart. Biochim. Biophys. Acta, **557**, 265-282 (1979).
- (7) A. Perelson. Exp. Cell Res., **112**, 309-321 (1978).
- (8) N. D. Gershon, A. Demsey and C. W. Stackpole. Exp. Cell Res., **122**, 115-126 (1979).
- (9) J. Markovics, L. Glass and G. G. Maul. Exp. Cell Res., **85**, 443-451 (1974).
- (10) S. Marcelja. Biochim. Biophys. Acta, **455**, 1-7 (1976).
- (11) S. Marcelja, D. J. Mitchell, B. W. Ninhan and M. J. Sculley. J. Chem. Soc., Faraday Trans. II, **73**, 630-648 (1977).
- (12) D. Marsh, A. Watts, R. D. Pates, R. Uhl, P. F. Knowles and M. Esmann. Biophys. J., **37**, 265-274 (1982).
- (13) T. Pearson and S. I. Chan. Biophys. J., **37**, 141-142 (1982).
- (14) F. Lado. J. Chem. Phys., **49**, 3092-3096 (1968).
- (15) B. A. Lewis and D. M. Engelman. J. Mol. Biol., **166**, 203-210 (1983).
- (16) K., S. Huang, H. Bayley and H. G. Khorana. Proc. Natl. Acad. Sci., U.S.A., **77**, 323-327 (1980).
- (17) L. Bachmann and W. W. Schmitt. Proc. Natl. Acad. Sci., U.S.A., **68**, 2149-2152 (1971).

- (18) Y. S. Chen and W. L. Hubbell. Exp. Eye Res., **17**, 517-532 (1973).
- (19) R. Peters and R. J. Cherry. Proc. Natl. Acad. Sci., U.S.A., **79**, 4317-4321 (1982).
- (20) J. Stamatoff, R. M. Lozier and S. Gruner. Methods Enzymol., **88**, 282-286 (1982).
- (21) V. A. Parsegian, N. Fuller and R. P. Rand. Proc. Natl. Acad. Sci., U.S.A., **76**, 2750-2754 (1979).
- (22) P. A. Baldwin and W. L. Hubbell. Biophys. J., **37** (2, Pt. 2); 85a (Abstr.) (1982).

CHAPTER 4

A Model for lipid Mediated Inter Protein
Interaction in Bilayer Membranes

Introduction

Many studies have shown that membrane proteins affect the behavior of neighboring lipids.¹⁻⁶ A related issue is the arrangement of protein particles among their neighbors, especially their tendency to cluster, even in the absence of cytoskeletal interactions.⁷⁻¹⁰ It has been proposed that the interaction between proteins is caused by their influence on lipids.¹¹⁻¹³ Evidence for a protein-protein interaction which is dependent on the lipid environment is seen in freeze-fracture studies of Chen and Hubbell¹⁴ and Lewis and Engelman,¹⁵ in which both bacteriorhodopsin and dark-adapted rhodopsin are seen to cluster when reconstituted into relatively thick phosphatidyl choline membranes.

In this chapter we present a model for the interaction of protein molecules in a lipid bilayer. We assume that a protein molecule is able to fit into the bilayer and thereby match its hydrophobic and hydrophilic regions with those of the surrounding lipids, but that this fitting causes some distortion of the protein-free equilibrium configuration of the bilayer and hence raises its energy relative to that equilibrium state. We derive an expression for the intermolecular potential energy arising from the perturbation of the lipid bilayer by the protein molecule.

A convenient test of the model is provided by measurement of the protein-protein pair distribution function from freeze-fracture micrographs of membrane systems which contain particles in a state of partial aggregation.^{7,16-18} The pair distribution function, $w(r, \Delta r)$, is given by the ratio of the density of particles in an annulus between r and $(r + \Delta r)$ nm from an average particle in the micrograph, to the overall

mean particle density. As aggregation standards, we have measured the particle pair distribution functions from pictures of Acholeplasma laidlawii membranes previously reported by James and Branton (1973). In Chapter 3 we showed that pair distribution functions derived from particles seen in freeze-fracture micrographs can be modeled using the relationship between the pair distribution function and the radial correlation function, $g(r)$, of a system of particles, namely:

$$w(r, \Delta r) = \frac{2 \int_r^{r + \Delta r} g(r) r \, dr}{\Delta r (2r + \Delta r)} \quad . \quad (1)$$

The radial correlation function can be calculated from the inter particle potential energy using published algorithms.¹⁸ The expression derived here for a lipid-mediated potential energy between particles can thus be used to model these measured functions. Our results suggest that aggregation state of particles in a membrane may be described by two parameters which are properties of the lipid phase and protein-lipid interaction, respectively.

Theory

Thermodynamics of Lipid Ordering. The most fundamental approach to protein-lipid interactions is via statistical mechanics. Although necessary to completely understand their interactions, it is inconvenient when analyzing their macroscopic behavior.

Here we resort to a thermodynamic model of the lipids. This approach allows us to study protein statistical mechanics via an

approximation of the lipid-mediated force by its mean value. We assume that the lipids have a degree of freedom, an order parameter, $\phi(\mathbf{r})$, which is a scalar function of position \mathbf{r} on the membrane surface and characterizes the lipid state at that point. The deviation of $\phi(\mathbf{r})$ from ϕ_0 , its value at unconstrained equilibrium, measures the extent of perturbation. We then express $f(\mathbf{r})$, the two-dimensional free energy density, as a function of $\phi(\mathbf{r})$ and $\nabla\phi(\mathbf{r})$:

$$f(\mathbf{r}) = f(\phi_0) + \epsilon(\phi, \nabla\phi) \quad (2)$$

where $\epsilon = 0$ when $\phi(\mathbf{r}) = \phi_0$ everywhere. We expand ϵ as a Taylor series around ϕ_0 .

$$\epsilon(\phi, \nabla\phi) = \epsilon = k_1 (\nabla\phi)^2 + k_2 (\phi - \phi_0)^2 + \dots \quad (3)$$

Linear terms would merely shift the equilibrium state, while higher-order terms preclude analytic solutions. The first term in equation 3 produces the cooperativity, an energetic cost for spatial variation of ϕ . The second term represents the restoring force tending to keep ϕ at its equilibrium value, ϕ_0 . Models based on the same idea have been developed by Marcelja,³³ Schroder,¹¹ Owicki et al.¹³ and Owicki and McConnell.¹² Equation 3 has also been used to describe protein effects on spin label partitioning.²⁰ We shall refer further to these works in the discussion.

Minimizing the total free energy yields the field equation:

$$\left(\frac{\nabla^2}{\eta^2} - 1 \right) \phi(\mathbf{r}) + \phi_0 = 0 \quad (4)$$

where $\eta^2 = k_2/k_1$. η^{-1} is a correlation length which always appears in combination with a spatial variable. Equation 4 can be solved for $\phi(\mathbf{r})$ using the appropriate boundary conditions corresponding to a given particle configuration. Substitution of $\phi(\mathbf{r})$ into equation 3 then yields an expression for the energy density $\epsilon(\phi, \nabla\phi)$ which can be integrated over the membrane area to obtain the energy of the particle configuration for which equation 4 was originally solved. Implicit in our approach is the assumption that η^{-1} for the lipids is a slowly varying function of the protein concentration. This should be a good approximation for the concentrations of proteins seen in the natural membranes studied here. However, it will be seen later that, in general, ϕ_0 , the equilibrium order parameter, needs to be replaced by a bulk order parameter averaged over the membrane and $\langle\phi\rangle$ is a function of lateral protein density.

We proceed to study the order parameter when there are one and two particles in the membrane. In both cases, the procedure is to solve equation 4, substitute $\phi(\mathbf{r})$ into equation 3, and integrate over the membrane to find the total energy. Its dependence on the arrangement of the particles reveals their interaction.

Single Particle Membrane Energy. Let ϕ be constrained to be $\bar{\phi}$ at the edge of a protein particle, which we assume to be circular with radius r_0 . The solution of equation 4 satisfying this and the requirement that $\phi(\mathbf{r}) = \phi_0$ at $r = \infty$ is:

$$\phi(r) = \phi_o + c_1 K_o(\eta r) \quad (5)$$

where $c_1 = (\bar{\phi} - \phi_o)/K_o(\eta r_o)$, K_n is a n^{th} order modified Bessel function of the second kind²¹ and r is the distance of r to the particle center.

The self-energy E_1 is the difference in order parameter (OP) energy between a membrane with one particle and one with none. The OP energy is zero in the absence of protein, so E_1 is found by substituting $\phi(r)$ into equation 3 and integrating over the membrane:

$$E_1 = c_1^2 k_1 \int_0^{2\pi} \int_{r_o}^{\infty} [(\nabla K_o(\sigma))^2 + K_o(\sigma)^2] \sigma d\sigma d\theta \quad (6)$$

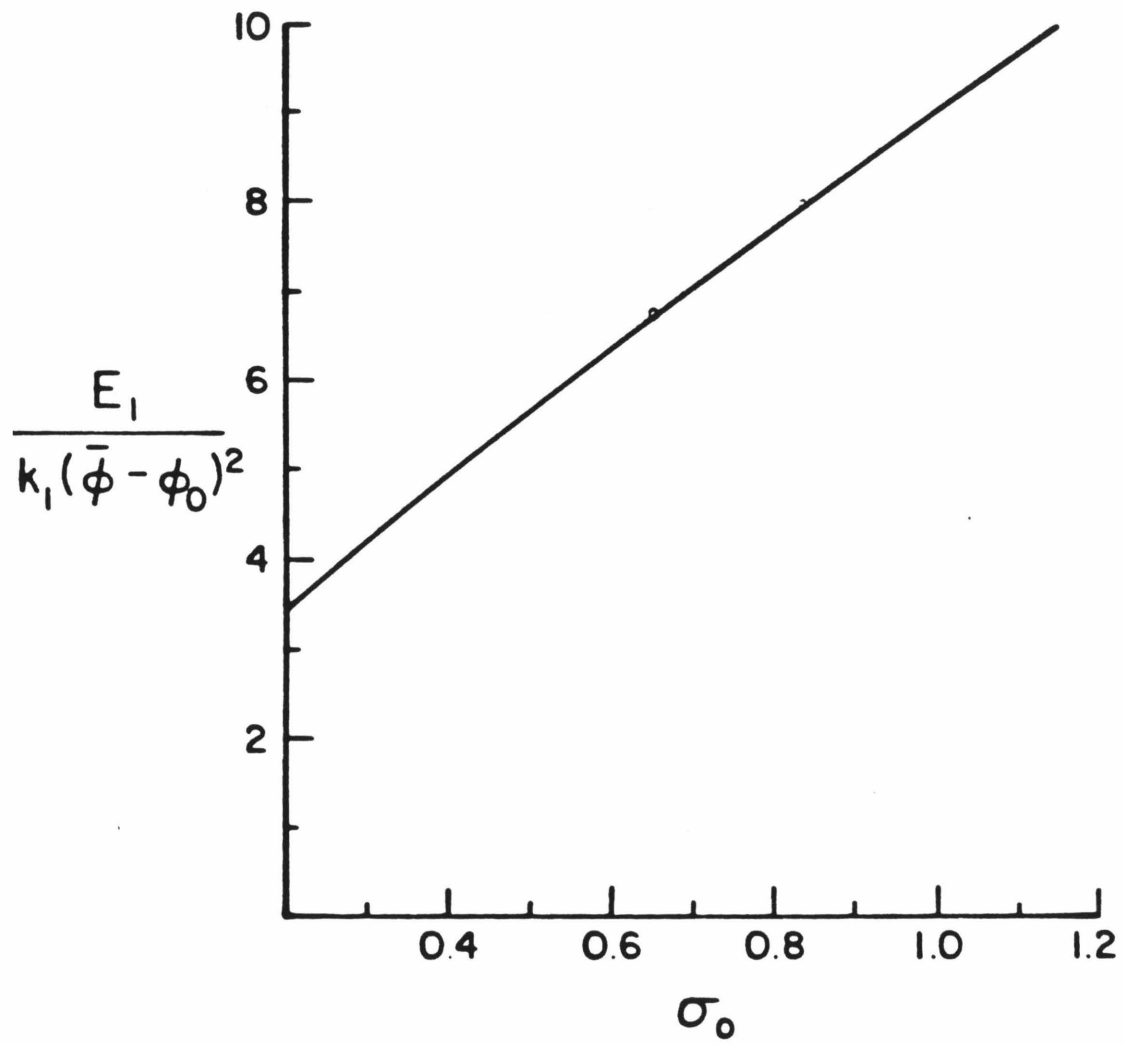
$$= 2\pi(\bar{\phi} - \phi_o)^2 k_1 \sigma_o K_1(\sigma_o)/K_o(\sigma_o) \quad (7)$$

where $\sigma = \eta r$, $\sigma_o = \eta r_o$, and ∇ now refers to σ rather than r .

E_1 appears repeatedly in our results. Its most obvious role follows from its definition. The change in OP energy when a particle moves from one lipid phase to another is the difference in E_1 between them. This is related to the standard free energy of transfer when the OP-independent interactions are the same in both phases. E_1 can thus control protein distribution between coexisting lipid phases. Figure 1 shows the dependence of E_1 on σ_o .

It has been assumed that the OP equals some constant

Figure 1. The dependence of the particle self-energy E_1 (expressed in units of $k_1 (\bar{\phi} - \phi_0)^2$) on the reduced particle size $\sigma_0 (\equiv \eta r_0)$.



$\bar{\phi}$ adjacent to the protein and that the direct constraining interactions do not extend away from the protein surface. In addition, the protein has been assumed to exert its influence along the perimeter of a circle. Although the latter assumption cannot be exact, we are concerned with mean behavior in regions larger than lipid molecules. Any shape irregularity would thus be smeared out. The model makes no assumption about the depth of the protein in the membrane since only two-dimensional structure is important.

Interaction Between Two Particles. The interaction between two protein particles in a membrane can be found by solving equation 4 when $\phi(\mathbf{r})$ is constrained to $\bar{\phi}$ at the boundaries of two particles. Consider a particle centered at the origin and one at $\mathbf{r} = \mathbf{r}'$. Outside the particles $\phi(\mathbf{r})$ is roughly:

$$\phi(\mathbf{r}) = \phi_0 + c_2(K_0(\eta r) + K_0(\eta|\mathbf{r}' - \mathbf{r}|)) \quad (8)$$

where

$$c_2 = (\bar{\phi} - \phi_0) / (K_0(\sigma') + K_0(\sigma_0)) . \quad (9)$$

This is inexact since $\phi(\mathbf{r})$ is not constant on the protein boundaries. Figure 2 shows the variation of $(\phi(\mathbf{r}_0) - \bar{\phi})/(\phi_0 - \bar{\phi})$ with θ , the angular coordinate of \mathbf{r}_0 on a protein perimeter. The distortion from circular symmetry is small so we neglect it here.

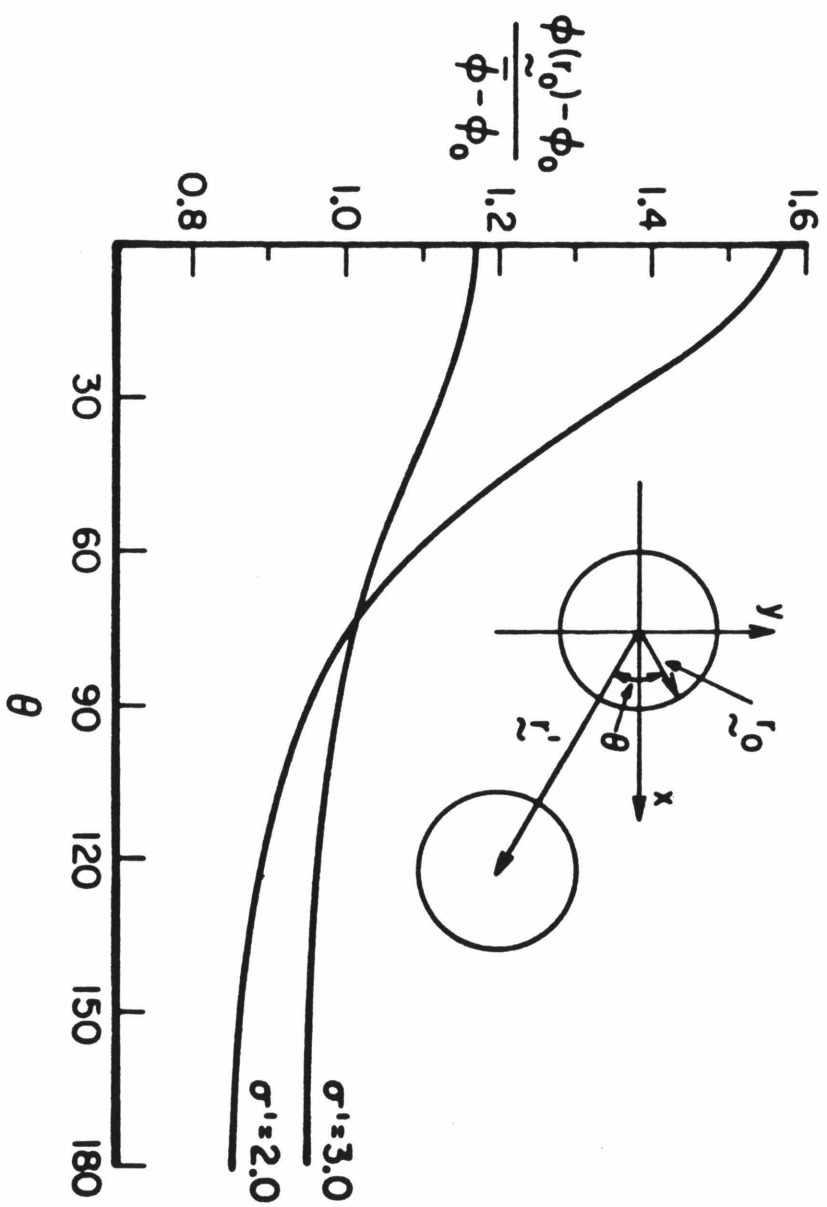
The two-particle OP energy, E_2 , is found by combining equations 3, 8 and 9:

Figure 2. In solving equation 4 for the two-particle problem, we invoke the circular boundary condition $\phi = \bar{\phi}$ at both particles. The solution given by equations 8 and 9 is therefore inexact. We illustrate here the departure from circular symmetry by comparing $\bar{\phi}$ with the exact $\phi(r_o)$. The dependence of

$$\frac{\phi(r_o) - \phi_o}{\bar{\phi} - \phi_o}$$

against θ is shown, where r_o is some point on the boundary of one particle, and θ is defined as in the diagram. The reduced particle size, σ_o is taken to be 1.0, and σ' , the inter particle separation, is 2.0 and 3.0. The circular boundary condition corresponds to

$$\frac{\phi(r_o) - \phi_o}{\bar{\phi} - \phi_o} = 1.0.$$



$$\begin{aligned}
 E_2 = c_2^2 k_1 \iint & (\nabla K_o(\sigma))^2 + (\nabla K_o(|\sigma - \sigma'|))^2 + 2 \nabla K_o(\sigma) \cdot \\
 & \nabla K_o(|\sigma - \sigma'|) + K_o(\sigma)^2 + K_o(|\sigma - \sigma'|)^2 + \\
 & 2 K_o(\sigma) K_o(|\sigma - \sigma'|) \sigma d\sigma d\theta
 \end{aligned} \quad (10)$$

which may be condensed into the less formidable result

$$2k_1 c_2^2 (M(0) + M(\sigma')) \quad (11)$$

using the definition:

$$M(\sigma') = \int_0^{2\pi} \int_{\sigma_o}^{\infty} A \sigma d\sigma d\theta - \int_0^{2\pi} \int_0^{\sigma_o} A \sigma d\sigma d\theta \quad (12)$$

and

$$A = \nabla K_o(\sigma) \cdot \nabla K_o(|\sigma - \sigma'|) + K_o(\sigma) K_o(|\sigma - \sigma'|). \quad (13)$$

The second term in M corrects for integrating the first over the interior of the particle at σ' . Equation 12 can be simplified with the following addition theorem (Gray, 1966):

$$\begin{aligned}
 K_o(|\sigma - \sigma'|) = \\
 I_o(\sigma) K_o(\sigma') + 2 \sum_{p=1}^{\infty} I_p(\sigma) K_p(\sigma') \cos p\gamma
 \end{aligned} \quad (14)$$

valid when $\sigma < \sigma'$. The region $\sigma > \sigma'$ is handled by interchanging σ and σ' . I_p is an order p modified Bessel function of the first type, and γ is the angle between σ and σ' . The summation drops out because the cosine integrates to zero. Carrying out the integration we find

$$M(\sigma') = 2\pi K_0(\sigma') (2\sigma_0 I_0(\sigma_0) K_1(\sigma_0) - 1). \quad (15)$$

When calculating $M(0)$, we make the approximation, justified later, of ignoring the second integral in equation 12 for $\sigma' = 0$ and obtain

$$M(0) = 2\pi\sigma_0 K_0(\sigma_0) K_1(\sigma_0) = E_1/k_1 c_1^2. \quad (16)$$

The lipid-mediated potential between the two particles is then:

$$\begin{aligned} V(\sigma') &= E_2 - 2E_1 \\ &= 2E_1 \left[\frac{1 + M(\sigma')/M(0)}{(1 + K_0(\sigma')/K_0(\sigma_0))^2} - 1 \right]. \end{aligned} \quad (17)$$

Figure 3 shows a plot of $V(\sigma')/E_1$ versus σ' , for various particle radii σ_0 or ηr_0 .

Finally, the integration leading to equation 16 includes the inside of the particle not centered on the coordinate origin. To estimate the error we evaluate the integral (see fig. 4):

Figure 3. Calculated two-particle potential energies (expressed in units of E_1) for various particle sizes ($\eta r_0 = 0.2, 0.5, 0.8$ and 1.1).

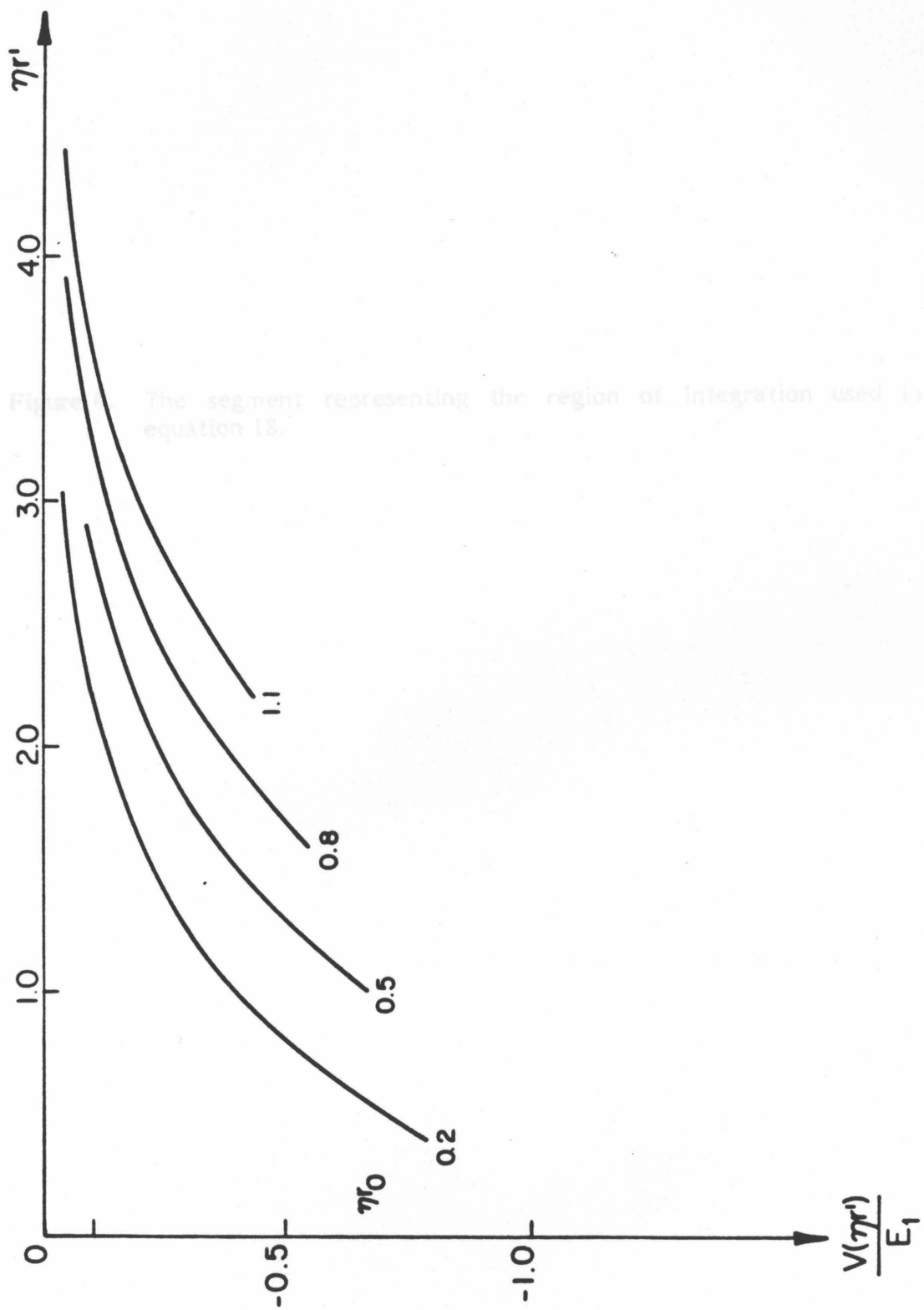
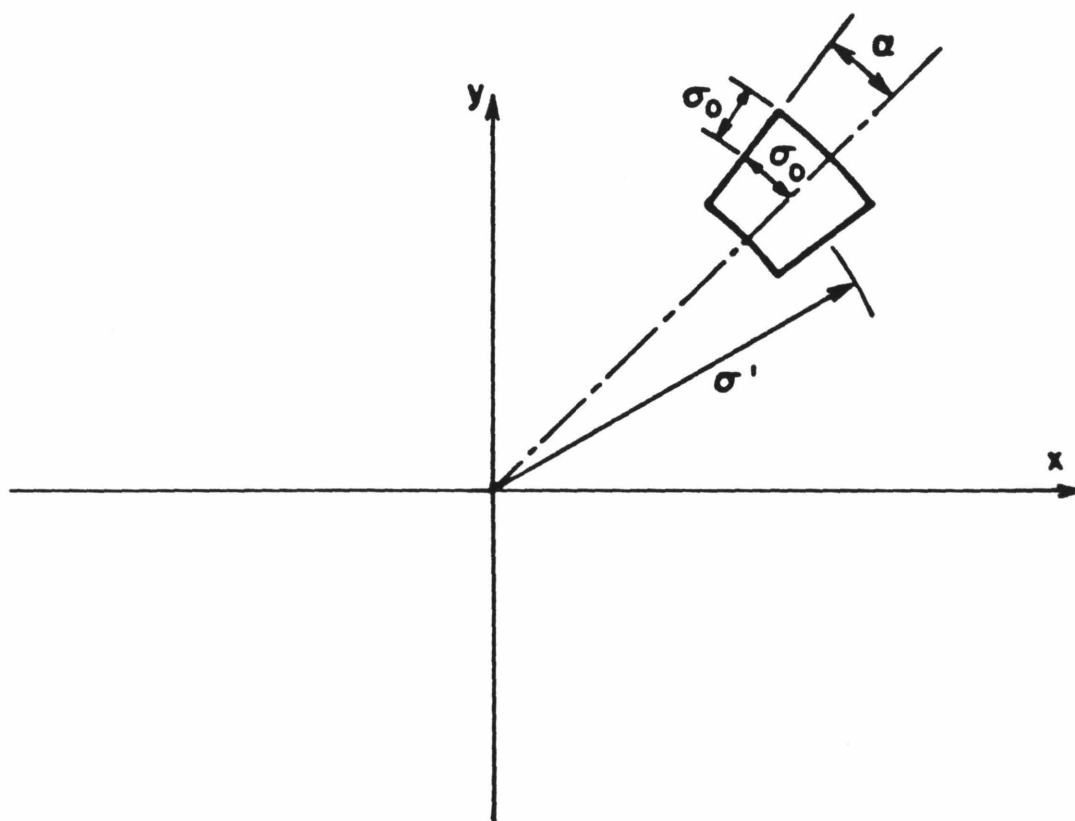


Figure 1. The segment representing the region of integration used in equation 1.8.

Figure 4. The segment representing the region of integration used in equation 18.



$$I^* = \int_{-\alpha}^{\alpha} \int_{\sigma' - \sigma_0}^{\sigma' + \sigma_0} (K_0^2(\sigma) + K_1^2(\sigma)) \sigma \, d\sigma \, d\gamma \quad (18)$$

$$= \frac{2\sigma_0}{\sigma'} \left[(\sigma' - \sigma_0) K_0(\sigma' - \sigma_0) K_1(\sigma' - \sigma_0) - (\sigma' + \sigma_0) K_0(\sigma' + \sigma_0) K_1(\sigma' + \sigma_0) \right] . \quad (19)$$

Table 1 shows values of σ' below which I^* exceeds 5% of $M(0)$ for values of $\sigma_0 = 0.2-2.0$. Since the particles do not interpenetrate, $\sigma' > 2\sigma_0$. It will be seen that σ_0 is typically about 1. The correction to $M(0)$ can thus be neglected.

Many particle Effects on the Order Parameter. The presence of other particles in the vicinity of a pair of interacting particles will have an effect on the magnitude of their interaction. This is because the presence of particles in the membrane will alter the bulk value of ϕ from ϕ_0 and will change the measure of the lipid-protein interaction. We quantify this effect by invoking the super-position approximation, i.e.,

$$\phi(\mathbf{r}) = \phi_0 + \sum_i c_N^i K_0(\eta|\mathbf{r}_i - \mathbf{r}|) . \quad (20)$$

When the particles are all identical, the boundary condition at particle j is roughly:

Table 1. Values of $\eta r'$ below which I^* exceeds 5% of $M(0)$.

ηr_0	$\eta r'$
0.2	0.52
0.5	1.36
0.8	2.00
1.1	2.64
1.4	3.26
1.7	3.70
2.0	4.60

$$\bar{\phi} - \phi_o = c_N^j K_o(\eta r_o) + \sum_{i \neq j} c_N^i K_o(\eta |r_j - r_i|) . \quad (21)$$

To find c , we assume that the membrane is homogeneous, so the neighbors of each particle are similarly arranged. The c 's are thus all about the same, and we assume them to be equal. Spatial variation of concentration is thereby ignored. Setting the c 's equal to c_N in equation 21, we solve for c_N :

$$c_N = \frac{\bar{\phi} - \phi_o}{K_o(\eta r_o) + \sum_{i \neq j} K_o(\eta |r_j - r_i|)} \quad (22)$$

We now replace $K_o(\eta |r_i - r_j|)$ by its mean value

$$\langle K_o(\eta |r_i - r_j|) \rangle \equiv \frac{2\pi}{N-1} \int_0^\infty g(r) K_o(\eta r) r dr ,$$

which may be readily integrated if we made the approximation $g(r) = 1.0$.

The outcome of this coarse graining is:

$$c_N = \frac{\bar{\phi} - \phi_o}{K_o(\sigma_o) + 4\pi(\rho/\eta^2) \sigma_o K_1(2\sigma_o)} \quad (23)$$

where ρ denotes the particle density.

Substituting this result into equation 20 yields, for the average value of ϕ :

$$\langle \phi \rangle = \phi_0 + c_N N \langle K_0 (|\sigma - \sigma_i|) \rangle, \quad (24)$$

where σ is any point not inside any particle. At sufficiently low particle densities $\langle \phi \rangle$ can be written as

$$\begin{aligned} \langle \phi \rangle &= \phi_0 + c_N 2\pi(\rho/\eta^2) \int_{\sigma_0}^{\infty} K_0(\sigma) \sigma d\sigma \\ &= \phi_0 + c_N 2\pi(\rho/\eta^2) \sigma_0 K_1(\sigma_0). \end{aligned} \quad (25)$$

Thus, in the many-particle problem, the interaction between any pair of particles is screened by their simultaneous interaction with all the others: (i) the effective bulk order parameter in the domain is increased from ϕ_0 to $\langle \phi \rangle$, and (ii) the effect of the lipid-protein interaction on the order parameter at the boundary of any protein molecule is reduced from $\bar{\phi} - \phi_0$ to $(\bar{\phi} - \phi_0)(1 - Y)$, where

$$Y = \frac{2\pi(\rho/\eta^2) \sigma_0 K_1(\sigma_0)}{K_0(\sigma_0) + 4\pi(\rho/\eta^2) \sigma_0 K_1(2\sigma_0)} \quad (26)$$

Since, in the two-particle problem (cf. equation 2) E_1 varies quadratically with $(\bar{\phi} - \phi_0)$, it follows that the intermolecular potential energy between any pair of protein molecules in the present case needs merely to be rescaled by a factor $(1 - Y)^2$ provided ρ is sufficiently low. Physical plausibility demands

that $Y < 1$.

Previous Work on Lipid-Mediated Interactions. We now compare our model of lipid-mediated protein-protein interactions with previous works. Earlier investigators predict, as we do, that proteins which perturb lipids tend to aggregate.

Marcelja³³ and Schroder¹¹ employ a mean field model to describe the behavior of a lipid order parameter, η . Marcelja assumes a hexagonal lattice for the lipids, wherein each site j is characterized by an order parameter η_j . Schroder assumes a lipid continuum and derives a differential equation for the change in order parameter $\delta\eta(\mathbf{r})$ away from the average value, η_0 , in the absence of the proteins. Both Marcelja and Schroder include the influence of proteins on the surrounding lipid by including a lipid-protein interaction term in an expression for the energy of the system. In both cases η is taken to be the average of the second-order Legendre polynomial:

$$\eta = \langle P_2(\nu) \rangle \quad (27)$$

where ν is an angle describing either lipid hydrocarbon chain or segment orientation. Schroder fixes the value of the order parameter at the protein-lipid boundary and solves for $\delta\eta(\mathbf{r})$ in the two-particle case, thereby deriving an expression for the inter-protein interaction energy. Marcelja solves for the order parameter self-consistently, and hence the inter-protein interaction energy, numerically. Neither author takes into account the saturation effect on the order parameter of protein particles in the vicinity of the two particles whose interaction is being considered.

Since we shall not attempt to give a molecular interpretation of the order parameter, introduced in the present work, further comparison with the work of Marcelja and Schroder must await further data on the nature and range of the order parameter mediating inter-protein interactions.

Pair Distribution Functions

Access to the two-particle inter particle potential of a system of particles, such as seen in a freeze-fracture micrograph, is provided in principle by measurement of the pair distribution function of the set of particles embedded in the membrane. For example, in Chapter 3 we showed that the PDF of a random distribution of protein could be simulated by assuming the proteins to be discs with no inter-protein interaction other than the hard repulsive core. The protein particles were modeled as if they were a two-dimensional fluid, and the PDF's were calculated using the Ornstein-Zernike equation:

$$g(r) = 1 + c(r) + \rho \int c(|r - s|) (g(s) - 1) d^2s. \quad (28)$$

$C(r)$ is the direct correlation function which as the particle densities studied here may be related to $g(r)$ by the Percus-Yevick relation:

$$c(r) = g(r) \{1 - \exp[V(r)/kT]\}. \quad (29)$$

This approach is quite general, and we wish now to test the attractive lipid-mediated potential derived here using these relations.

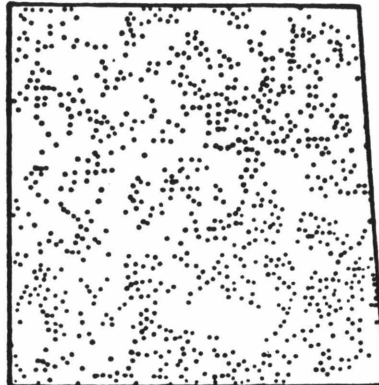
An attractive inter particle potential energy would be seen in a freeze-fracture micrograph as partial aggregation of the particles. A convenient set of micrographs of partially aggregated systems is that published in figure 1 of James and Branton.²² These authors selected five systems ranging from random to completely aggregated as aggregation standards in a study of the effect of lipid composition on particle distribution in Acholeplasma laidlawii membranes. We present particle patterns obtained from their figure 1 in figure 5. However, in order for the measured PDF to represent an intermolecular potential energy function in the context in which we present it here, it is assumed that the membrane, although partially aggregated, is still homogeneous. There must be no phase separation, either of one lipid phase from another, or of the protein from the lipid phase. Accordingly, from the work of James and Branton, we limit ourselves to a consideration of figures 1a, 1b and 1c, in which protein particles appear throughout the membrane. Figure 1e seems to show complete separation of either a lipid phase or the protein phase from the lipid. We discuss later in this chapter the problems that may be associated with using a natural membrane systems for these measurements.

The PDF for each micrograph was determined by placing the micrograph on a Tektronix graphic tablet and recording the coordinates of each particle in the plane of the picture. The annulus size (Δr in equation 1) was 10 nm. These measured PDF's were then simulated using the lipid-mediated potential energy, equation 17, as the inter particle potential energy in equation 29. The many-particle correction, equation 26 was included. Equations 28 and 29 were solved for $g(r)$ using the algorithm of

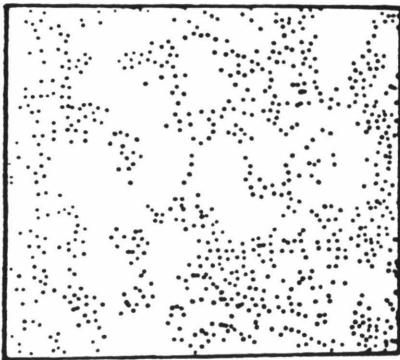
Figure 5. Computer-generated representation of the particle distributions in the EM pictures taken from figure 1 of James and Branton (1973).



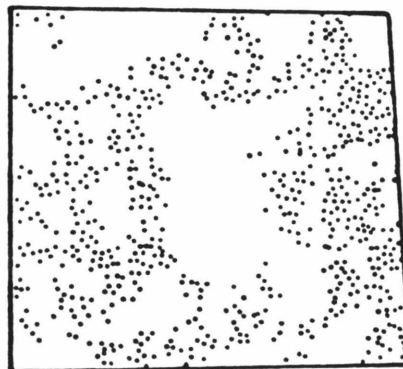
A



B



C



D



E

200 NM

Lado,¹⁹ and the PDF, $w(r, \Delta r)$, was calculated from $g(r)$ using equation 1. The procedure used for simulation entailed adjusting η^{-1} , the correlation length, until the rate of decay of the calculated PDF from its peak was similar to that of the measured function, and then adjusting the protein-lipid interaction energy, $k_1 - (\phi_0 - \phi)^2$, until a fit was obtained as judged visually. An empirical observation which aided the fitting was that η^{-1} for a measured PDF was approximately the distance required for the PDF to decay by one-half from its peak value.

In figure 6(a-c) we show PDF's of the systems of James and Branton (1973) under consideration here. Table 2 summarizes the parameters that give the best fits. The correlation lengths appear to be between 5 and 10 nm for the partially aggregated membranes. Figure 1a of James and Branton is consistent with a PDF (our figure 6a) with the freeze-fracture particles being randomly diffusing hard discs. The increasing aggregation state upon going from figure 1a to 1c can be modeled by increasing lipid correlation length and protein-lipid interaction energy.

Discussion

Lewis and Engelman¹⁵ have studied the effect of lipid hydrocarbon chain length on the state of aggregation of bacteriorhodopsin reconstituted into phosphatidyl choline of various hydrocarbon chain lengths. If bacteriorhodopsin is reconstituted into thin phosphatidyl choline bilayers such that the boundary layer of lipids is capable of stretching to accommodate the protein, then the protein adopts a random arrangement in the plane of the

Figure 6. Measured (+) and simulated (-) PDF's for the particle distributions in figures 1a-c of James and Branton (1973). $\Delta r = 10$ nm. a) $\rho = 0.0032 \text{ nm}^{-2}$, $r_0 = 5.0$; b) $\rho = 0.0025 \text{ nm}^{-2}$, $r_0 = 4.0$ nm; c) $\rho = 0.0025 \text{ nm}^{-2}$, $r_0 = 4.0$ nm.

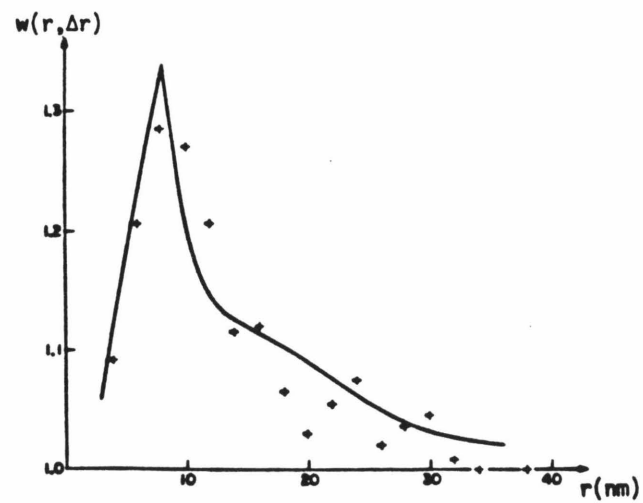
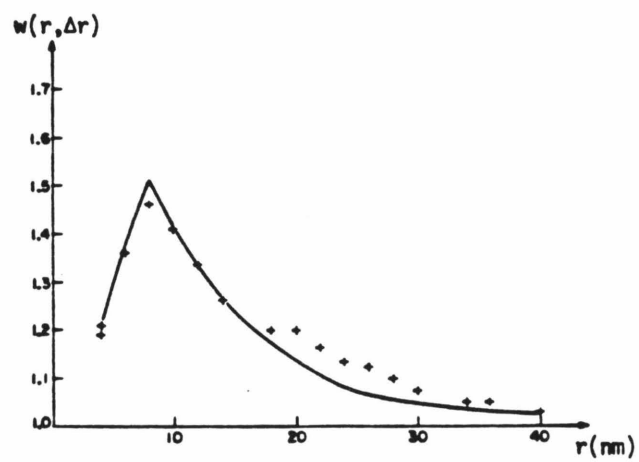
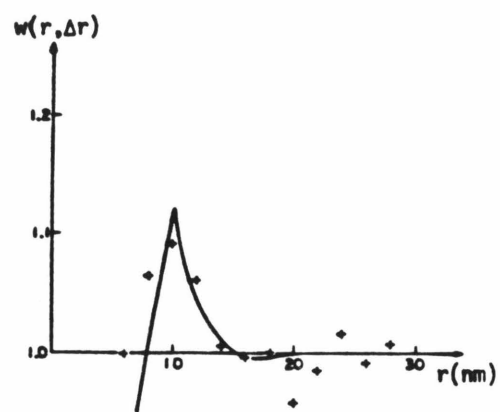


Table 2. Parameters used in simulating particle distribution functions.

EM Picture	$k_1 D^2$	E_1	η^{-1}	r_o
James and Branton (1973)	(kT)	(kT)	(nm)	(nm)
Figure 1a	0.0	--	--	5.0
Figure 1b	0.65	4.5	6	4.0
Figure 1c	1.30	6.4	10	4.0

membrane (Chapter 3). In a situation where lipids and proteins in a bilayer are unable to match their hydrophilic and hydrophobic surfaces, separation of the protein phase from the lipid phase occurs. Thus separation is manifested in freeze-fracture micrographs as aggregation of the protein particles.

In cases where the lipid hydrophobic surface is thicker than that of the protein, both random and aggregated protein states are seen. Perturbation of the lipid by the protein can be short ranged or extend further into the bilayer. If the lipid adjusts its length by changing the number of gauche bonds per hydrocarbon chain, then the perturbation would be expected to be short-ranged.¹⁷ An alternative mechanism by which a thick bilayer may accommodate the protein is lipid tilt. Tilt distortions would be expected to be longer ranged, by analogy with similar distortions seen in liquid crystals.²³ Tilting of the lipid molecules may therefore produce an interaction between protein molecules.²⁴ Partial or total aggregation of the protein molecules would then be a consequence of propagation laterally through the bilayer of the tilt distortion at the protein-lipid boundary.

The protein-protein PDF therefore contains information about the extent of the protein-lipid interaction and its propagation through the bilayer. In the present work, we present a theory which allows us to gain some insights into these issues from PDF's measured from freeze-fracture electron micrographs. Our results show, for example, that it is possible to simulate very closely the PDF's from partially aggregated A. laidlawii membranes using a model with essentially two adjustable parameters: (i) the correlation length, η^{-1} , which is a property of the lipid phase and describes the distance over which the order parameter affecting protein distribution is

propagated in that phase; and (ii) the protein-lipid interaction energy, $k_1(\bar{\phi} - \phi_0)^2$, which provides a measure of the protein-lipid interaction at the protein-lipid boundary. Other parameters in the inter-protein potential, namely r_0 and p , can be deduced directly from a measured PDF and the freeze-fracture micrograph, respectively.

Given the assumptions that we have made so far, and despite the crudity of our model, the observed PDF's of A. laidlawii membranes are well simulated by the potential energy function of equation 17, taking into account the correction to equation 17 described by equation 26. Such a simulation is obviously not unique, and there may be other potential energy functions which provide equally close fits to the measured functions. However, it is difficult to see what other mechanisms would provide such a long-range attraction, in particular since the attraction has to be a function of lipid composition.

The principal assumption that we make in calculating the pair distribution function from the particle coordinates taken from a freeze-fracture picture is that the protein-lipid system is a single phase. This assumption implies that the protein does not separate from the lipid phase and that one lipid phase does not separate from another. This is a hard assumption to justify on the basis of a freeze-fracture picture since the freeze-fracture process is taking, as it were, a "still" picture of a dynamic system. Further work is necessary to ascertain unambiguously whether partially aggregated systems such as those used in the study by James and Branton and referenced here do, in fact, consist of a single homogeneous phase.

The possibility of artifacts due of the A. laidlawii membranes being a mixture of different lipid and protein species must be considered. The fact that a natural membrane consists of a mixture of lipids does not necessarily invalidate or approach. We have used a mean-field theory to model protein membrane interactions. We assume a single correlation length is an average property of the lipid phase irrespective of whether the membrane lipids are one pure chemical species or a mixture. This assumption seems to be justified by the large magnitude of the correlation lengths obtained relative to the molecular size of the lipids in the plane of the membrane.

The possibility that the particles are not all of the one protein species is a more serious objection to the use of a natural membrane system in the context of measurement of PDF's. Such inhomogeneity may be manifested as variations among the particles in r_0 and $(\bar{\phi} - \phi_0)$. Inhomogeneity in r_0 would cause broadening in the PDF. Comparison of the calculated PDF using a random hard-disc model and that measured from figure 1a of James and Branton shows that, in fact, there is little broadening in the PDF except for some flattening of the top of the peak. The values of $r_0 = 5.0$ nm and $\rho = 0.0032$ nm⁻² are entirely consistent with a model in which all the protein particles in that picture are randomly diffusing hard discs.

Particle inhomogeneity would not cause the increase in peak size on going from figure 1a to 1c. This, we propose, must be a lipid-mediated effect. If this is the case, the peak size is largely governed by the magnitude of the protein-lipid interaction and in the case of a natural membrane will be simply an average of that interaction over all the protein particles.

In cases where there is a hard-disc repulsion between particles and no

other type of repulsive interaction the position of the peak in the radial correlation function, and hence the pair distribution function, is a measure of $2r_0$. The measured values of r_0 consistent with peak position for particles in the A. laidlawii membranes of James and Branton are 4.0 nm in the partially aggregated membranes and 5.0 nm for particles in the random distribution of figure 1a. The reduction of r_0 on going from figure 1a to 1b and c is consistent with the appearance of the particles in the photographs. Particles appear to be somewhat smaller in figure 1b than in 1a. It is not possible to tell at this point whether this represents a genuine conformational change in the membrane proteins or is an artifact in the freeze-fracture process caused by the change in lipid composition. However, in all the pictures we have analyzed so far, the position of the peak in the PDF is consistent with the radius of particles estimated from the pictures.

One parameter of particular importance is the self energy, E_1 , of the protein. E_1 is defined by equation 6 and represents the energy cost of placing a protein particle into the bilayer. We have so far assumed the lipids to be uniform. When they separate into two phases, preferential incorporation of protein into one of the phases would resemble precipitation. For instance, Cherry, et al.³⁶ have shown that bacteriorhodopsin in lecithin precipitates when cholesterol is added. The phase behavior of lecithin and cholesterol is only beginning to be understood. However, they form a two-phase system under many conditions.³⁵ In terms of our model, a large difference of E_1 between the two phases would appear as precipitation. Alternatively, cholesterol could raise E_1 or the lipid correlation length, thus causing protein precipitation. This latter mechanism could also account for the

bacteriorhodopsin aggregation in ordered lipid phases³⁴ and in nature.^{37,38} The value of E_1 depends on $(\bar{\phi} - \phi_0)^2$. Adjusting $(\bar{\phi} - \phi_0)$ may therefore be a mechanism for controlling the state of aggregation of membrane-bound proteins and hence their interaction. One way of changing $(\bar{\phi} - \phi_0)$ is via the protein. This could account for aggregation induced by proteolysis^{39,40} ligand binding^{41,42} or rhodopsin dark adaptation.¹⁴ Another way to change $(\bar{\phi} - \phi_0)$ is via the lipids. Examples of this may be provided by drugs, such as primaricin, nystatin, and amphotericin B, which bind to the lipids and also cause protein aggregation.²⁵ Phospholipases^{26,27} and lipid phase transitions³⁴ can also make the proteins aggregate. Cross-linking agents, such as antibodies and lecithins²⁸⁻³² can also precipitate proteins by producing additional attractions between them. The dependence of protein aggregation on the membrane state is further evidence that it is not just an artifact of freezing.

References and Notes

- (1) D. F. H. Wallach, S. P. Verma and J. Fookson. Biochim. Biophys. Acta, **559**, 153-208 (1979).
- (2) L. Mateu, F. Caron, V. Luzzati and A. Billecocq. Biochim. Biophys. Acta, **508**, 109-121 (1978).
- (3) B. M. Moore, B. R. Lentz and G. Meissner. Biochemistry, **17**, 5248-5255 (1978).
- (4) A. Watts, I. D. Volotovski and D. Marsh. Biochemistry, **18**, 5006-5013 (1979).
- (5) J. Davoust, A. Bienvenue, P. Fellman and P. F. Devaux. Biochim. Biophys. Acta, **596**, 28-42 (1979).
- (6) D. Chapman, B. A. Cornell, A. W. Eliazs and A. Perry. J. Mol. Biol., **113**, 517-538 (1977).
- (7) R. P. Pearson, S. W. Hui and T. P. Stewart. Biochim. Biophys. Acta, **557**, 265-282 (1979).
- (8) T. P. Copps, W. S. Chelack and A. Petkau. J. Ultrastruc. Res., **55**, 1-3 (1976).
- (9) J. Melborn and L. Packer. Biophys. J., **16**, 613-625 (1976).
- (10) L. Finegold. Biochim. Biophys. Acta, **448**, 393-398 (1976).
- (11) H. Schroder. J. Chem. Phys., **67**, 1617-1619 (1977).
- (12) J. C. Owicki and H. M. McConnell. Proc. Natl. Acad. Sci., U.S.A., **76**, 4750-4754 (1979).
- (13) J. C. Owicki, H. W. Springgate and H. M. McConnell. Proc. Natl. Acad. Sci., U.S.A., **75**, 1616-1619 (1978).
- (14) Y. S. Chen and W. L. Hubbell. Exp. Eye Res., **17**, 517-532 (1973).

- (15) B. A. Lewis and D. M. Engelman. J. Mol. Biol., **166**, 203-210 (1983).
- (16) N. D. Gershon, A. Demsey and C. W. Stackpole. Exp. Cell Res., **122**, 115-126 (1979).
- (17) L. T. Pearson, B. A. Lewis, D. M. Engelman and S. I. Chan. Biophys. J., **43**, 167-174 (1983).
- (18) J. T. Donnell and L. X. Finegold. Biophys. J., **35**, 783-798 (1981).
- (19) F. Lado. J. Chem. Phys., **49**, 3092-3096 (1968).
- (20) W. Kleeman and H. M. McConnell. Biochim. Biophys. Acta, **419**, 206-222 (1976).
- (21) A. Gray. "A Treatise on Bessel Functions"; Chapter 3; Dover Publications: New York, 1966.
- (22) R. James and D. Branton. Biochim. Biophys. Acta, **323**, 378-390 (1973).
- (23) P. G. DeGennes. "The Physics of Liquid Crystals"; Oxford University Press: Oxford, 1974.
- (24) B. A. Cornell, J. B. Davenport and F. Separovic. Biochim. Biophys. Acta, **689**, 337-345 (1982).
- (25) Y. Kitajima, T. Sekiya and Y. Nozawa. Biochim. Biophys. Acta, **455**, 452-465 (1976).
- (26) A. J. Verkleij, R. F. A. Zwaal, B. Roelofsen, P. Comifurius, D. Kastelijm and L. L. M. Van Deenen. Biochim. Biophys. Acta, **323**, 178-193 (1973).
- (27) J. Olive, E. L. Benedetti, P. J. G. M. Van Breugel, F. J. M. Daemen and S. L. Bonting. Biochim. Biophys. Acta, **509**, 129-135 (1978).
- (28) T. L. Steck. J. Cell Biol., **62**, 1-19 (1974).

- (29) G. M. Edelman. Science, **192**, 218-226 (1976).
- (30) G. L. Nicholson. Biochim. Biophys. Acta, **457**, 57-108 (1976).
- (31) C. DeLisi and A. Perelson. J. Th. Biol., **62**, 159-210 (1976).
- (32) G. R. Schreiner and E. R. Unanue. Adv. Immunol., **24**, 37-165 (1976).
- (33) S. Marcelja. Biochim. Biophys. Acta, **455**, 1-7 (1976).
- (34) R. J. Cherry, V. Muller, R. Henderson and M. P. Heyn. J. Mol. Biol., **121**, 283-298 (1978).
- (35) B. R. Lentz, D. A. Barrow and M. Hoechli. Biochemistry, **19**, 1943-1954 (1980).
- (36) R. J. Cherry, V. Muller, G. Hohenstein and M. P. Heyn. Biochim. Biophys. Acta, **596**, 145-151 (1980).
- (37) R. Henderson. Ann. Rev. Biophys. Bioeng., **6**, 87-109 (1977).
- (38) R. Casadio and W. Stoeckenius. Biochemistry, **19**, 3374-3381 (1980).
- (39) D. Branton. Phil. Trans. Roy. Soc. London, **B261**, 133-138 (1971).
- (40) V. Speth, D. F. H. Wallace, E. Weidekamm and H. Knufferman. Biochim. Biophys. Acta, **255**, 386-394 (1972).
- (41) R. B. Gunn and R. G. Kirk. J. Mem. Biol., **27**, 265-282 (1976).
- (42) C. R. Kahn. J. Cell Biol., **70**, 261-286 (1976).

CHAPTER 5

A Study of the Organization of Cytochrome c Oxidase in Lipid Bilayers

Introduction

In order for a protein molecule to intercalate successfully into a lipid bilayer, the bilayer must match its hydrophilic and hydrophobic regions with the corresponding region on the protein molecules.¹ The bilayer may alter its equilibrium (protein-free) state to accommodate protein by a number of mechanisms that may involve changes in the conformation or configuration of head group or hydrocarbon regions. For example, thickening of the bilayer may be a result of an increase in the number of trans conformers per hydrocarbon chain. Other alterations in bilayer structure may be a result of lipid tilt.²⁻⁴

In the past few years, there have been a number of studies published that model theoretically the effect of protein molecules which are embedded in lipid bilayer membranes on both the membrane and, in some cases, the protein distribution.^{3,5-11} All of these studies have in common that a parameter which is a property of the membrane is chosen, and the effect of the protein on the free energy of the membrane through the effect of the protein on the selected parameter is modeled. The work of Marcelja,⁵ Schroder,⁶ Markin,¹⁰ and Pearson et al.³ indicates that an inter-protein force, most likely manifested as aggregation of protein molecules, is a result of perturbation of membrane by protein and is an indicator of protein-lipid interaction.

The kind of intramolecular conformation change that is required for example in thickening of the bilayer to fit a protein does not appear to induce a long-ranged interaction between protein molecules.² This result confirms the theoretical predictions in this regard by Marcelja.⁵ However, as pointed

out by Gruler and Sackmann,¹¹ lipid tilt may induce longer-ranged interactions.

We have previously modeled the long-ranged interaction that induces partial aggregation in membrane by assuming that the energy density on a membrane surface is a simple harmonic function of the gradient of some order parameter and the deviation of the order parameter about some equilibrium configuration,³ namely:

$$\epsilon(\mathbf{r}) = k_1 (\nabla\phi)^2 + k_2 (\phi(\mathbf{r}) - \phi_0)^2 + \dots \quad (1)$$

This level of approximation always produces an attractive potential between protein particles if it is assumed that the order parameter is assigned a fixed value at the protein-lipid boundary. For relatively small perturbation of the bilayer by the protein, such an approximation may be expected to hold. A more complete treatment, however, requires the introduction of terms to third and fourth order in $(\phi(\mathbf{r}) - \phi_0)$, as pointed out by Owicki et al.⁷ For example, a more severe perturbation of the lipid by the protein may be expected to change the value of k_2 in equation 1, making it a function of ϕ (equivalent to including higher-order terms) and thereby inducing what may be termed a protein-mediated lipid-mediated inter-protein interaction. Such an interaction may ultimately be repulsive and bring about a dispersion of protein particles. The possibility of such an effect was hinted at by Markin,¹⁰ who pointed out that a difference in curvature between protein and membrane may result in aggregation of protein in patches, but if the patch is

stiffer than the surrounding membrane, there will be a repulsion between particles within the patch.

It should be possible, in order to test the validity of the concepts of membrane structure expressed above, to examine the aggregation behavior of a protein that has been reconstituted into a lipid bilayer. In particular, it is appropriate to use a protein which is known to present an asymmetric surface to surrounding lipid and therefore would be expected to induce structural changes in the bilayer.

In the present work we have chosen to use cytochrome c oxidase in bilayers of dimyristoyl phosphatidyl choline (DMPC), dimyristoyl phosphatidyl glycerol (DMPG) and cardiolipin (CL). Cytochrome c oxidase appears to be asymmetrically (noncylindrically) shaped¹⁷ and has been shown to incorporate preferentially into vesicles of diameter 22-40 nm.¹² DMPC, DMPG and CL do not have spontaneous curvatures this large, and it may therefore be expected that there is a mismatch between protein and lipid that may induce lipid-mediated interactions between protein molecules.

In order to study lipid-induced protein interactions, we utilize an approach developed previously^{2,3} of measuring pair distribution functions (PDF's) of protein clusters seen by freeze-fracture electron microscopy (FFEM) and quantitating the inter-protein potential energy from the measured PDF. We find that the forces between protein molecules are more complex than the simple lipid-mediated attractive force previously postulated^{3,5,6} and that there appears to be, in addition, a lipid-mediated long-range repulsion between particles.

Very similar results to ours appear to have been obtained very recently

by Braun, et al.¹³ with mouse liver gap-junction protein. In the discussion section, we shall elucidate further on a proposed mechanism to explain our results.

Materials and Methods

Preparation of Protein-Lipid Recombinants. Beef heart cytochrome c oxidase was isolated by the procedures of Hartzell and Reinert¹⁴ and stored in 1% cholate buffer (10 mM tris, pH 7.4) at -85°C until used. For reconstitution, 100 μ L of oxidase/cholate stock solution at \sim 2.5 mg/mL protein concentration was added to 10 mg lipid (DMPC, CL or DMPG) that had been taken up in 1 mL of 1% cholate, 10 mM tris, pH 7.4. The detergent/protein lipid mixture was dialyzed against 1 ℓ of buffer (10 mM tris, with 1 M NaCl being optional) plus 20 g Amberlite XAD-2 resin. Dialysis was carried out for at least 54 h with at least six changes of buffer plus resin.¹⁵ The resulting recombinant was either fractured fresh or stored at -85°C before fracturing. Storage had no effect on the micrographs that were obtained. DMPC and DMPG were purchased from Calbiochem, CL from Sigma. Lipids were used as received without further purification.

Freeze-Fracturing. A sample of 1.5 μ L was loaded between 25 μ m thick copper discs and frozen from 300 K in Freon 22 with no fixative or cryoprotectant. Fracturing took place at -100°C in Balzers BA 360 M at 10^{-6} torr, and fractured samples were etched for 20 sec with a knife at -180°C. The fractured and etched specimens were shadowed using a quartz crystal to monitor Pt thickness, then coated with carbon.

Replicas were removed from the copper discs using ~ 4 M nitric acid and rinsed in bleach for an hour and then overnight in distilled water. The washed replicas were picked up onto formvar-coated grids (Pelco) and observed in a Phillips EM 201c electron microscope at 80 kV.

Pair Distribution Functions. The PDF, denoted $w(r, \Delta r)$, represents the ratio of the density of freeze-fracture particles in an annulus from r to $r + \Delta r$ nm from an average particle, to the mean density of particles in a region of membrane. If $w(r, \Delta r) < 1.0$, depletion in particle density, and hence a repulsive interaction between particles, is indicated. The nature of inter particle forces, whether repulsive or attractive, for a range of inter particle distances can be determined using the PDF. Regions of membrane that contained particles were photographed, and if the particle number (N) in a region were greater than about 300, then particle positions were digitized on a graphics tablet (Tekronix, Inc.) and the PDF calculated as described previously.^{2,3}

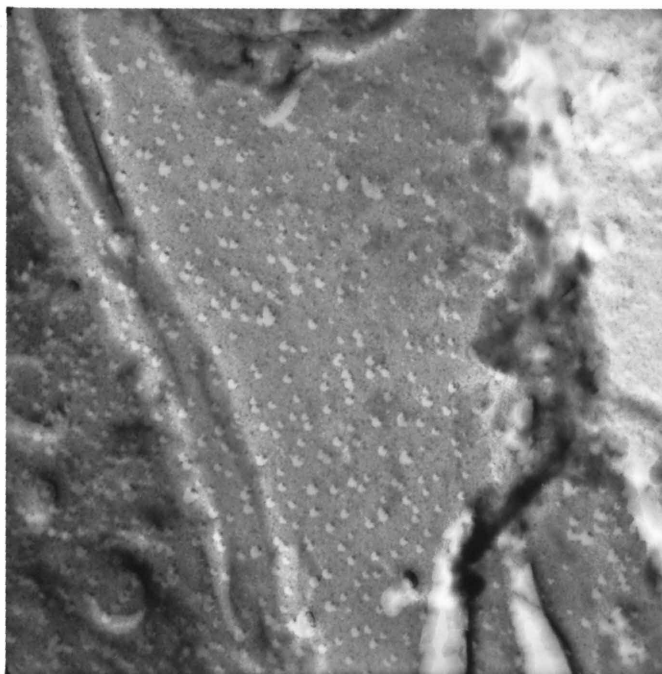
Results

In figure 1a-d we show representative micrographs of cytochrome oxidase in DMPC at low salt and 1 M NaCl, in cardiolipin and in DMPG, respectively. In the oxidase/DMPC, low-salt recombinant regions were seen which had the appearance of particles but no membrane. These are consistent with previously published micrographs of oxidase in water suspension.¹⁶ We show an example of such a region in figure 2.

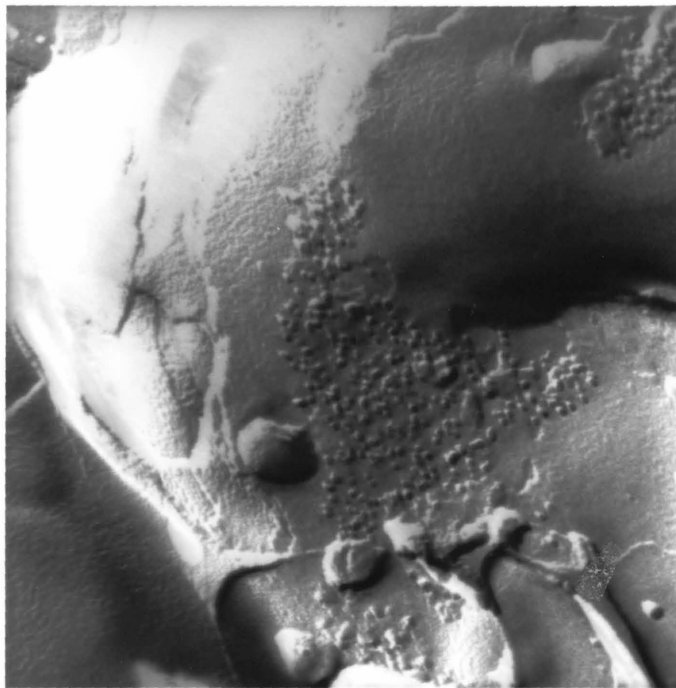
In cases where there was clearly bilayer membrane with protein

Figure 1. Freeze-fracture micrographs of cytochrome c oxidase particles in lipid bilayer membranes. Buffer in each case except b) was 0.01 tris, pH 7.4. a) In DMPC. b) in DMPC, plus 1 M sodium chloride. c) In cardiolipin. d) In DMPG. The bar on each photograph represents 100 nm.

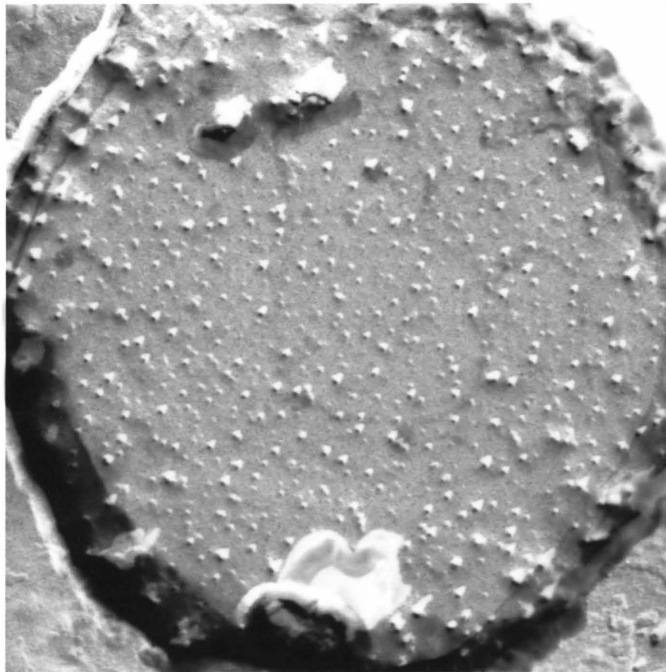
(a)



(b)



(c)



(d)

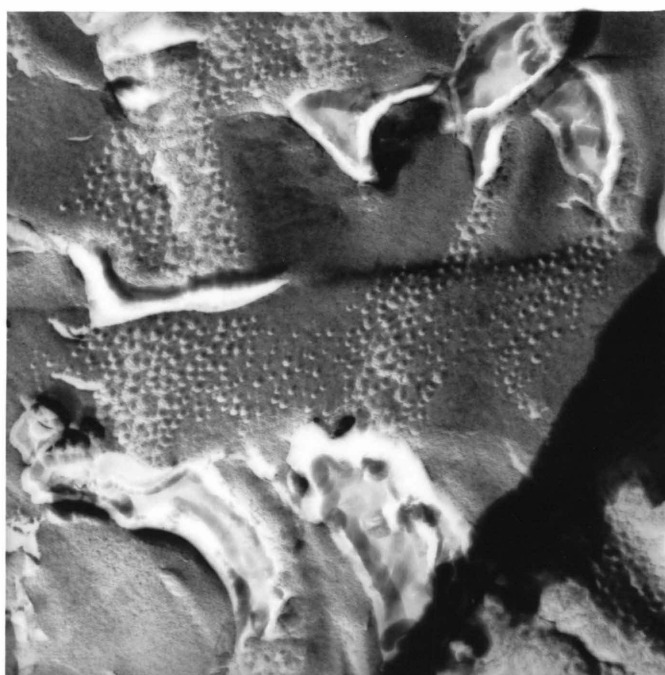


Figure 2. Micrograph of a structure seen commonly in the oxidase/DMPC low-salt sample. Particles are not intercalated into a bilayer and may represent protein in aqueous suspension or protein-lipid complexes into high protein:lipid mole ratio.

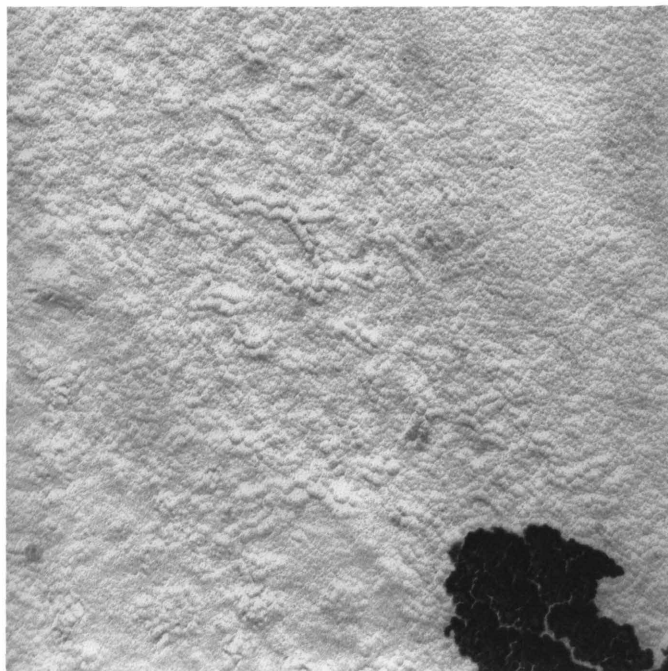
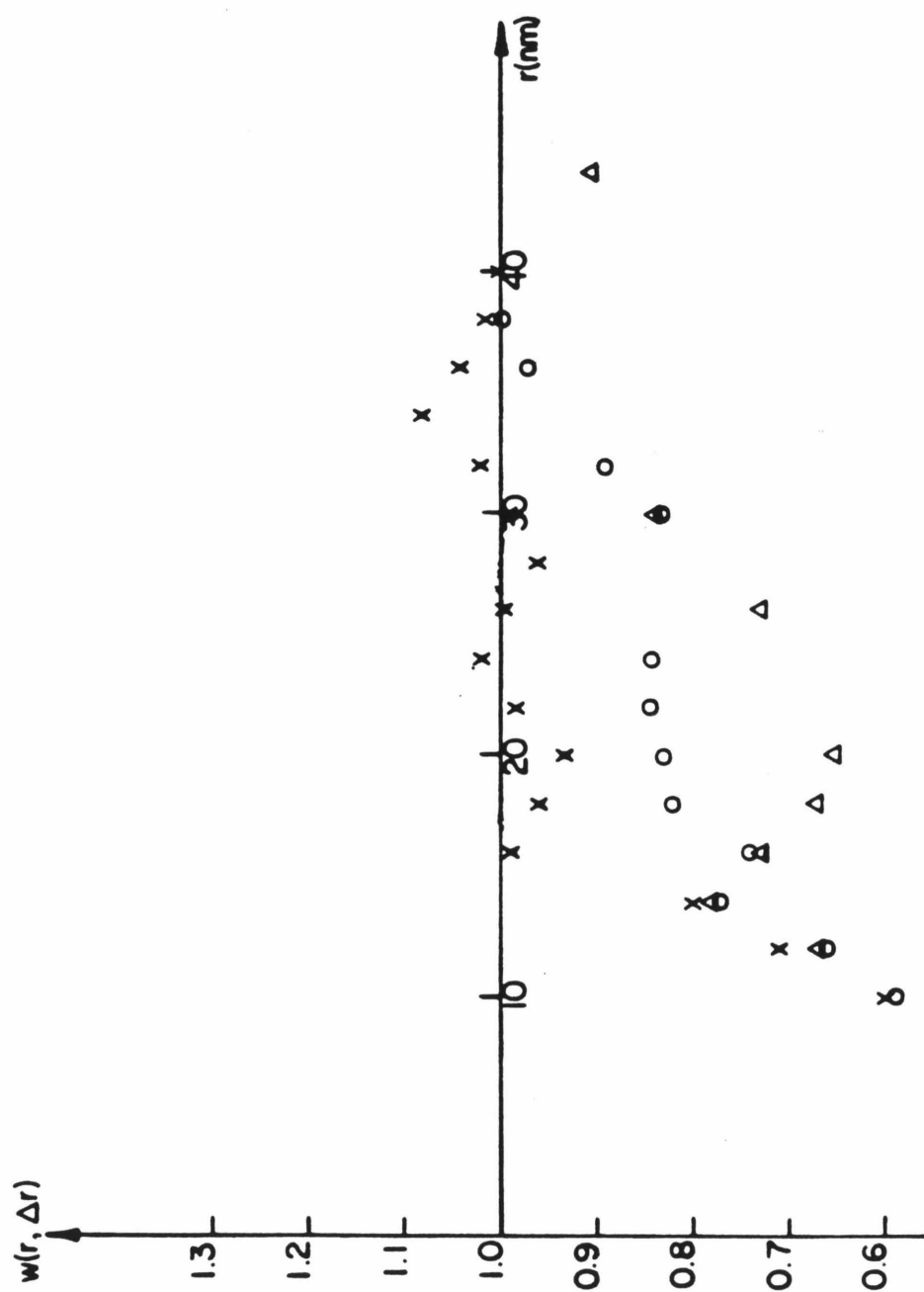
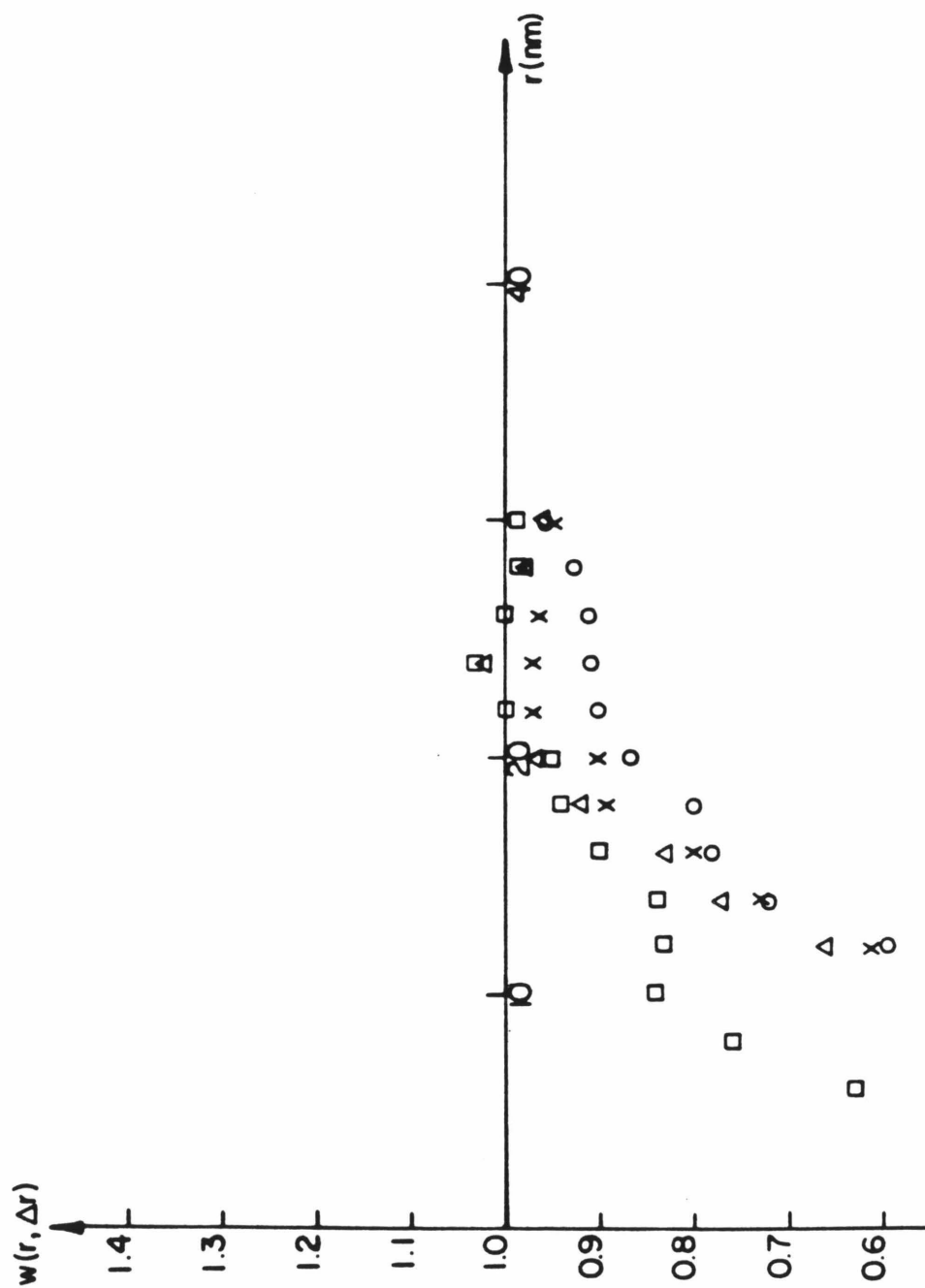


Figure 3. PDF's of cytochrome c oxidase in lipid bilayer membranes. The number of particles per membrane ranged from 300-500. a) in DMPC, low-salt sample. b) In DMPC, 1 M sodium chloride. c) In cardiolipin. d) In DMPG.

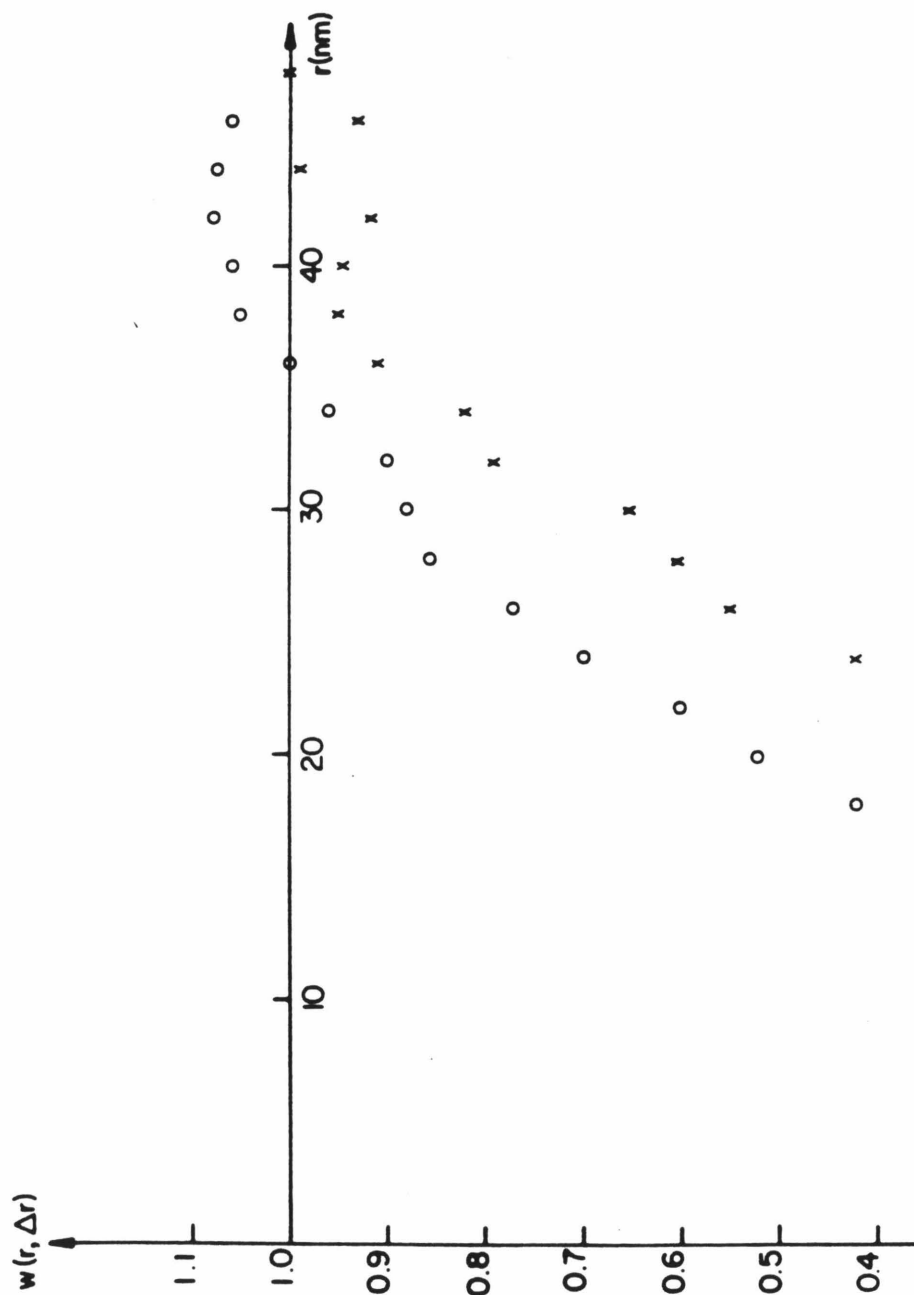
(a)



(b)



(c)



(d)

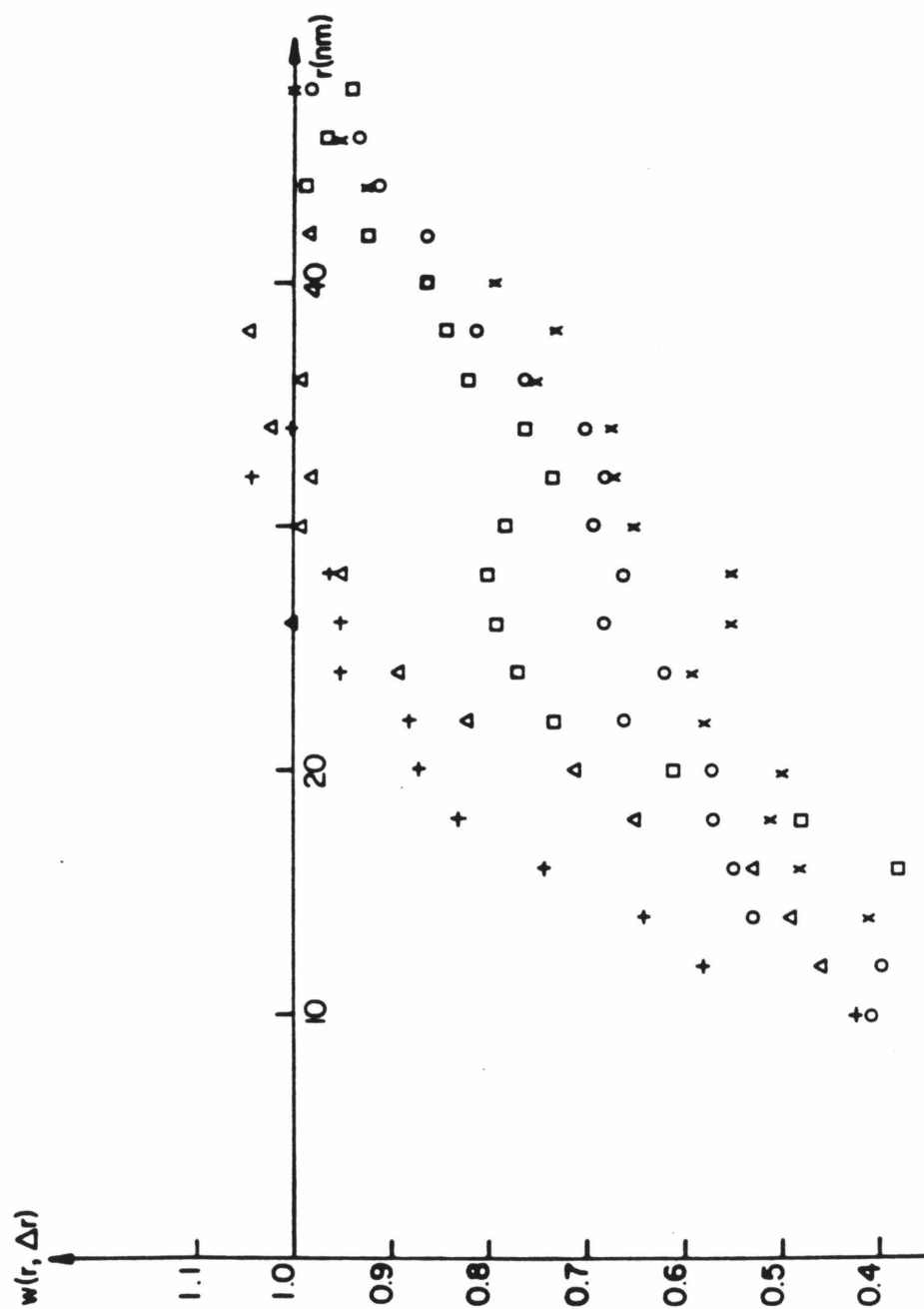


Table 1

Sample	ρ_{an} (nm ⁻²)	Comments
Oxidase + DMPC (low salt)	0.00044	Large areas of protein-free membrane, plus areas of particles that appeared unreconstituted.
Oxidase + DMPC (1.0 M salt)	0.0013	Large areas of protein-free membrane. Oxidase appeared ordered into patches.
Oxidase + Cardiolipin	0.00059	Large areas of protein-free membrane with some particle-containing areas.
Oxidase + DMPG	0.00039	As with oxidase + cardiolipin sample.

particles, the PDF of the particles was measured. Figure 3a-d shows the measured PDF's. In Table 1 we summarize the appearance of each sample, and list the average particle densities that were obtained. The solubility of oxidase in DMPC at low salt was very low. Large areas of membrane contained no particles, and those areas where particles were found contained relatively few particles. Measurements of particle density and PDF's were consequently difficult and could be made from only a limited number of membranes. Generally, each symbol on the diagrams in figure 3 represents one membrane.

In DMPC both high and low salt, the PDF's are characteristic of a long-range repulsion. The oxidase in cardiolipin also reconstitutes to a low lateral density, and the repulsion between particles as shown by the PDF is even more pronounced than in DMPC (fig. 3c). For some membranes the PDF does not reach 1.0 until r is above 40 nm. It is tempting to postulate that the longer-ranged repulsion in cardiolipin over DMPC is due to the significantly larger cross-sectional area of the cardiolipin molecule compared to that of the DMPC molecule. However, in figure 3d we show the PDF's for the oxidase/DMPG recombinant where the longer-ranged repulsion between particles persists.

Discussion

We have examined in this chapter the effect of lipid composition on the distribution of cytochrome c oxidase in protein-lipid recombinants. In a medium of low (0.01 M) ionic strength the protein is only sparingly soluble in DMPC as judged by FFEM. This result is consistent with that of earlier

workers.¹² The PDF of the protein particles is suggestive of a long-ranged repulsion. In DMPG and CL and in DMPC at high ionic strength the protein forms patches and the PDF of protein within these patches is still indicative of a repulsive interaction. This result is seemingly in contradiction to the attractive interaction that would be necessary to cause aggregation into patches.

If the repulsion that is seen in the protein/DMPC recombinants at low ionic strength is due to electrostatic interactions between charges on the hydrophilic surface of the protein, then one might expect that shielding of such repulsion would occur at high ionic strength and the PDF would reflect an essentially random distribution. The persistence of a repulsion within the patches of protein requires an explanation and we examine here the possibility that lipid mediated effects may bring about a repulsion.

In our previous treatment of lipid-mediated protein interactions (Chapter 4) we considered the inter-protein potential energy to be given by:

$$V(r') = E_2(r'/\xi) - 2E_1(\xi)$$

where ξ is a correlation length $(= (k_1/k_2)^{1/2})$ from equation 1, r' is the inter particle separation and E_2 and E_1 are the energies of two and one particles, respectively, in a bilayer membrane. E_2 and E_1 are derived from equation 1 by constraining the value of $\bar{\psi}$ to be $\bar{\psi}$ at the boundaries of two or one particles of radius r_0 . In the approximation of equation 1, $V(r')$ is always attractive. However, we wish to consider the possibility that if protein perturbs lipid bilayers to such an extent that ξ is changed by the protein,

then inter particle repulsion may result.

One crude way to illustrate this possibility is to replace ξ by $\langle \xi \rangle_{r'}$, where the average refers to the average value of ξ in a region of membrane between two particles that are separated by a distance r' . The inter particle energy is then:

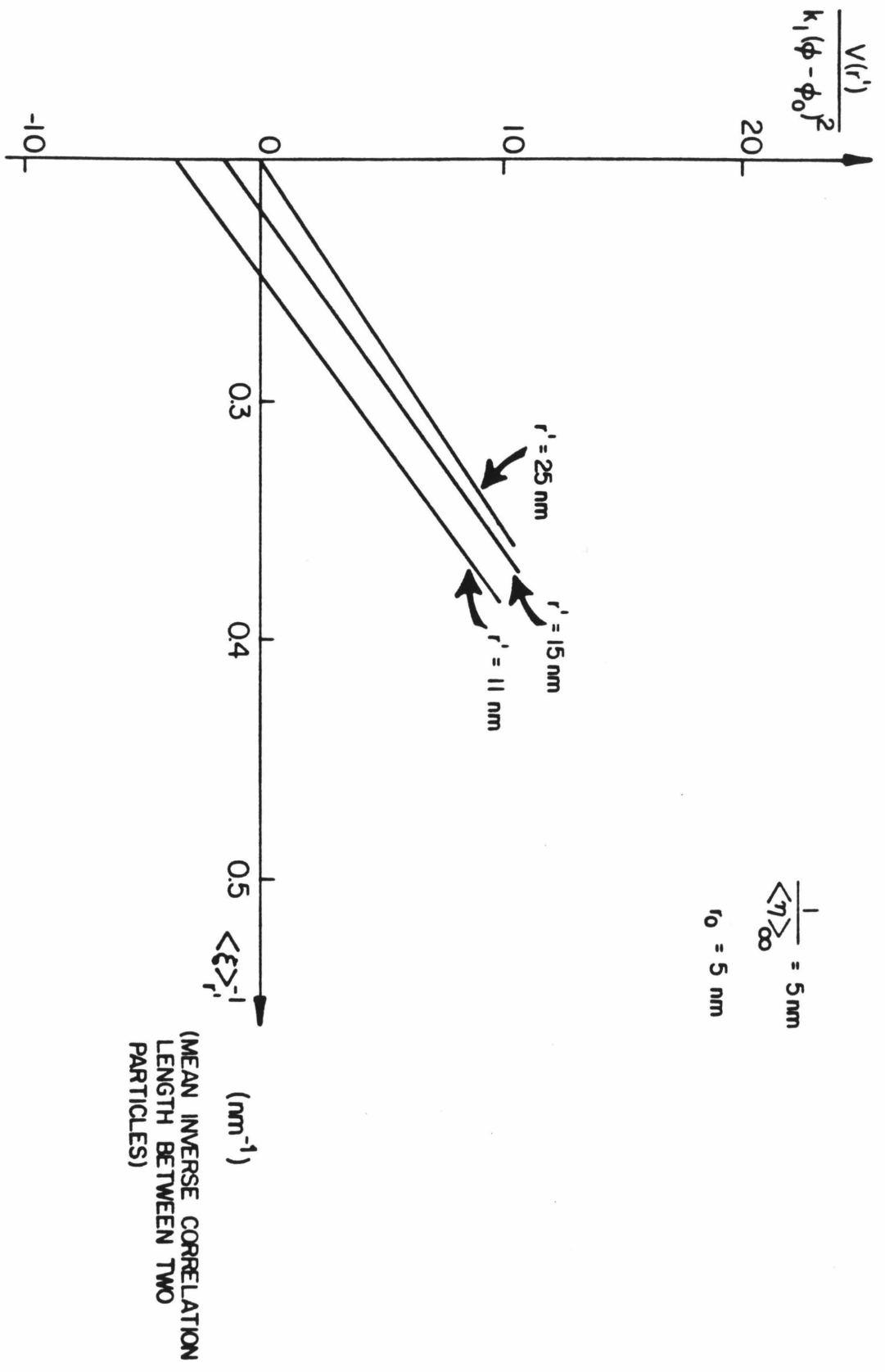
$$V(r') = E_2(r' / \langle \xi \rangle_{r'}) - 2E_1(\langle \xi \rangle_{\infty})$$

where $\langle \xi \rangle_{\infty}$ is the average correlation length for the membrane in the presence of two particles which are infinitely separated. In figure 4 we illustrate the behavior of $V(r')$ with changes in $\langle \xi \rangle_{r'}^{-1}$ for a case where $r_0 = 5 \text{ nm}$ and $\langle \xi \rangle_{\infty} = 5 \text{ nm}$. We have used the expressions for E_2 and E_1 derived in Chapter 4. The units of $V(r')$ are $k_1(\bar{\Phi} - \phi_0)^2$, which is typically 1 kT for a membrane in which partial aggregation is manifested.³ Each line in figure 4 represents one value of r' , the inter particle separation, and therefore only one point on each line represents a point on the actual inter particle potential energy curve. The full inter particle potential energy curve will be given by a curve connecting points on each of the lines that are shown.

The treatment that gives rise to figure 4 is admittedly crude and is intended only to show that a small change in $\langle \xi \rangle_{r'}$, for example, from 5 nm to 4 nm in our example, can give rise to a repulsive interaction for appropriate values of r' .

Reducing $\langle \xi \rangle_{r'}$ is equivalent to raising k_2 in the inter particle region if k_1 is kept constant. The alternative mechanism of reducing k_1 to reduce

Figure 4. A plot of $V(r)/k_1(\phi_0 - \bar{\phi})^2$ against the mean inverse correlation length of the bilayer between two particles $\langle \xi \rangle_{r'}^{-1}$. Each line applies to a single inter particle distance r' .



$\langle \xi \rangle_{r'}$ is possible, although the fact that $V(r')$ has a close to linear dependence on $\langle \xi \rangle_{r'}$ results in a $k_1^{1/2}$ dependence of $V(r')$. Reducing k_1 therefore reduces the magnitude of $V(r')$ and we will focus on mechanisms for changing k_2 .

Our model for protein-lipid interactions is based on an expansion of the free energy density to only second order in an order parameter. Models have been published of lipid bilayer order which utilize the full Landau expansion of free energy density.^{7,9} In the Landau expansion, terms to third and fourth order in $(\phi - \phi_0)$ are included. The free-energy density then becomes:⁹

$$\begin{aligned} \varepsilon(\mathbf{r}) = & k_1 (\nabla \phi)^2 + k'_2 (\phi - \phi_0)^2 \\ & - k'_3 (\phi - \phi_0)^3 + k'_4 (\phi - \phi_0)^4 \end{aligned} \quad (2)$$

where we have used the prime on the k 's to denote that they refer to the fourth, rather than the second, order expansion. Recalling equation 1:

$$\varepsilon(\mathbf{r}) = k_1 (\nabla \phi)^2 + k_2 (\phi - \phi_0)^2 \quad (1)$$

it can be seen that the k' factors in equation 2 are simply coefficients in a Taylor series expansion of k_2 about ϕ_0 . Therefore, k_2 may be altered by the protein perturbing ϕ away from ϕ_0 sufficiently that the higher order terms in $(\phi - \phi_0)$ must be invoked. However, the qualitative behavior of equation 2, plotted for example by Jahnig,⁹ indicates

that inclusion of k'_3 and k'_4 has the effect of reducing the contribution of terms in $(\phi - \phi_0)^n$ to the free-energy density, and hence reducing k_2 . It therefore seems unlikely that an inter particle repulsion would result from a change in k_2 arising from the additional terms in $(\phi - \phi_0)^2$ in equation 2 over equation 1. We therefore turn to other mechanisms for a repulsion.

We can hypothesize two different explanations for the existence of an apparently repulsive interaction between protein particles. The first, and simplest, is that protein is simply solidifying lipid in the protein-rich patches into a gel phase and protein particles can therefore no longer be modeled by a two-dimensional liquid theory. The repulsion in this case is only apparent and is due to lipid molecules in the gel phase separating protein particles.

The second mechanism involves what amounts to a change in k_2 by the introduction of a second parameter that describes lipid order, in this case represented by a vector field over the membrane surface.

The possibility of solidification of lipids in protein patches does in fact arise from equation 2 and has been pointed out by Owicki and McConnell.¹⁸ These authors have carried out calculations of lipid order in the presence of a two-dimensional hexagonal protein lattice, and show that at sufficiently high protein density a liquid crystalline to gel phase transition can be induced by protein if the protein tends to order the lipid at its boundary that would otherwise be in the liquid crystalline state.

If solidification of lipid is taking place, then immobilization of the protein would be a result, and testing of the above hypothesis should be straightforward using techniques to examine protein and lipid mobility. For

example, Swanson et al.¹⁹ have studied the rotational mobility of cytochrome oxidase reconstituted with mitochondrial lipids or with asolectin using a cholate dialysis procedure. Aggregation into patches of the protein is observed as evidenced by a relatively large (~ 1 mS) correlation time for protein rotation. The immediate lipid vicinity around the protein is shown to be viscous, but not solid. The presence of any lateral mobility in the protein would, however, imply that our measured PDF's represent a true inter particle potential energy and not merely freezing of protein particle positions.

The motional state of lipids in the presence of cytochrome oxidase has been extensively studied by ^2H nuclear magnetic resonance spectroscopy (NMR) and electron paramagnetic resonance spectroscopy (EPR) of appropriately labeled lipids.²⁰⁻²² By NMR, a separate gel phase component of the lipid in cytochrome oxidase/DMPC recombinants is not seen.²⁰ An exchange rate of $\geq 10^3 \text{ s}^{-1}$ between mobile and "immobile" lipid is therefore implied. This figure is consistent with EPR data from recombinants in which a spin labeled DMPC is used.²³ Knowles et al.²³ have also pointed out that their EPR data is consistent with some immobilization of boundary lipid extending beyond the first lipid shell around the protein with exchange taking place between shells, and some formation under certain circumstances of protein rich patches. "Immobilization" as used in the context of EPR on lipid spin labels actually appears to refer to slowing but not stopping of lipid motions. The notion of frozen protein + lipid patches within cytochrome oxidase/lipid recombinants, as we have hypothesized that notion here, is probably therefore not an accurate one.

Further insight may be provided by studies using differential scanning calorimetry (DSC). Rigell and Freire²⁴ and Chen and Friar²⁵ have recently reported such studies on cytochrome oxidase/DMPC recombinant. Both groups report seeing the main DMPC transition, but there is also a second phase transition that appears above the normal gel to liquid crystal phase transition of DMPC. Rigell and Freire estimate that 99 lipid molecules per protein molecule are removed from the main DMPC transition and that the second, higher, transition involves the protein. It may be that the second transition represents a protein + lipid transition within the protein-rich region of the bilayer. Further analysis awaits full publication of these authors' results. However, the figure of 99 lipid molecules per protein molecule leads to a very much higher particle density than we observed here if it is assumed that these 99 lipid molecules per protein molecule comprise the lipid content of the patches that we observe.

There is a more subtle possible explanation for the origin of the repulsion that we observe that allows for the protein and lipid to be fluid within the protein-rich patches. Theories of bilayer membrane structure are often based on theories of order in nematic or smectic liquid crystals. For example, Jahnig⁹ uses as an order parameter in equation 2 the symmetric, traceless second-rank tensor given by:²⁶

$$S_{ij} = S(r) (\delta_{ij} - 3n_i(r)n_j(r)) \quad (3)$$

where n_i are the components of a unit vector giving the direction of the axis of molecules at r . Free-energy density is given in terms of S instead of

$(\phi - \phi_0)$.

A full description of liquid crystalline behavior would also include terms which describe the elastic energy associated with changes in molecular orientation. In the case where all the Frank elastic constants are equal (the "one constant" approximation)²⁷ this means using an expansion of the free-energy density of the type:

$$F = F_0 + 3AS^2 - 2BS^3 + 9CS^4 + 3D(\nabla S)^2 + 9DS^2((\text{div} \cdot \mathbf{n})^2 + \text{curl} \mathbf{n})^2 \quad (4)$$

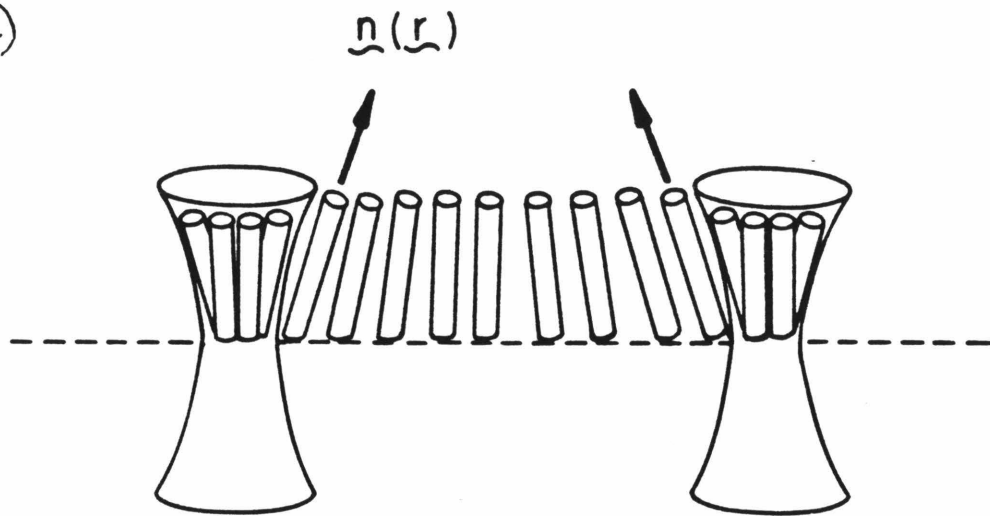
where we have retained the notation of constants used by Fan and Stephen²⁶ and F now refers to a free-energy density per unit volume whereas in our original treatment ϵ referred to free energy per unit area.

The last term in equation 4 includes the spatial rate of change of molecular orientation of lipid molecules. In a situation in which protein molecules induce a twist (i.e., $\text{curl } \mathbf{n} \neq 0$) or a splay ($\text{div} \cdot \mathbf{n} \neq 0$) configuration to adjacent lipid molecules, then the close approach of two protein molecules could become energetically expensive. In order to accommodate both protein molecules within a smaller membrane area lipid molecules would be required to undergo spatially more rapid changes in orientation.

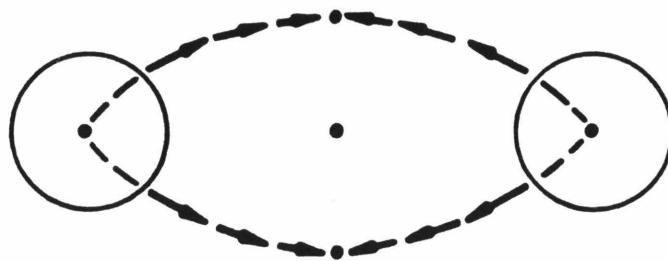
In figure 5a we illustrate the hypothesis for a case where protein molecules induce splay in boundary lipid. In figure 5b the length of the arrow indicates the deviation from the membrane normal of lipid molecules. From figure 5b it can be seen that a twist ($\text{curl } \mathbf{n} \neq 0$) is also induced when the two

Figure 5. a) Splay distortion in lipid bilayer structure at a protein lipid boundary can be propagated into the bulk of the lipid. b) The effect of splay distortions at protein lipid boundary producing a $\text{curl } \mathbf{n} \neq 0$ condition as two protein molecules approach. The length of the arrows represents the projection of the lipid orientation vector onto the membrane surface.

a)



b)



protein molecules approach each other.

A mechanism similar to that which we are proposing here has been proposed by Gruler and Sackmann,¹¹ who base their proposal on the properties of Schlieren textures in nematic and smectic liquid crystals.²⁸ These authors pointed out that if protein induces splay distortions in neighboring lipid, then an inter-protein repulsion results if two protein molecules approach each other that induce the splay in the same sense. This model is equivalent to the picture of figure 5, and our results represent the first experimental demonstration of this repulsion.

The induction of tilt in molecules in a smectic A liquid crystal produces the smectic C phase. The smectic A to smectic C transition has been induced by compression of a smectic A phase. The protein molecules in a bilayer may be envisaged as inducing tilt locally by compression of the membrane at the protein lipid boundary. We can estimate the energy cost of such a compression using a typical value of one of the elastic constants of 10^{-6} dyne cm^2 for a liquid crystal.

The two-dimensional Frank constant, K' , is given by $K' = Kd$ where d is the width of a bilayer. Taking $d = 3$ nm yields a value for K' of 3×10^{-20} J nm^2 , which is around 8 (kT) nm^2 at $T = 300$ K. We have previously shown that perturbations at the protein lipid boundary of the order of 1 kT can cause changes in the protein state that are manifested in deviations of the protein particle PDF from a random model.

Considering equation 1, if ϕ represents membrane thickness, then a value of $k_1(\bar{\phi} - \phi_0)^2$ of 1 kT implies that $k_2 \sim 8$ (kT) nm^2 for $\bar{\phi} - \phi_0 = 0.36$ nm, where $\bar{\phi} - \phi_0$ represents the change in

membrane thickness between the protein-lipid boundary and the bulk lipid. That protein can remain dispersed under this boundary condition has been shown by Lewis and Engelman, who demonstrated that bacteriorhodopsin remains dispersed in lipid bilayers up to 0.4 nm thicker than the thickness of the protein. The value of K' that is typical for liquid crystals, if used for bilayer membranes, is realistic for protein both to remain dispersed and yet also be affected in its distribution by lipid mediated effects.

Close approach of protein molecules would bring about, in equation 4, an increase in the term in S^2 , equivalent to an increase in k_2 in our notation. As was pointed out above, increase in k_2 can bring about an energy cost which results in a repulsion between particles. At sufficiently large inter particle distances the effect of splay and twist may be negligible enough that the attractive interaction predicted for equation 2 dominates and produces aggregation of particles into the protein-rich patches that we observe. The net particle distribution represents a balance between opposing forces and the particle density and PDF contain information about the various constants appearing in equation 4. It seems likely that a full numerical analysis of equation 4 in conjunction with freeze-fracture data and spectroscopic measurements on the disposition of lipid adjacent to protein should yield quantitative data on the elastic constraints of lipid bilayers and the way these affect and are affected by protein.

Referneces and Notes

- (1) B. A. Lewis and D. M. Engelman. J. Mol. Biol., **166**, 203-210 (1983).
- (2) L. T. Pearson, B. A. Lewis, D. M. Engelman and S. I. Chan. Biophys. J., **43**, 167-174 (1983).
- (3) L. T. Pearson, J. Edelman and S. I. Chan. Biophys. J., in press (1984).
- (4) W. Helfrich. Z. Naturforsch., **28c**, 693-703 (1973).
- (5) S. Marcelja. Biochim. Biophys. Acta, **455**, 1-7 (1976).
- (6) H. Schroder. J. Chem. Phys., **67**, 1617-1619 (1977).
- (7) J. C. Owicki, M. W. Springate and H. M. McConnell. Proc. Natl. Acad. Sci., U.S.A., **75**, 1616-1619 (1978).
- (8) E. M. B. DeLacey and J. Wolfe. Biochim. Biophys. Acta, **692**, 425-430 (1982).
- (9) F. Jahnig. Biophys. J., **36**, 329-345 (1981).
- (10) V. Markin. Biophys. J., **36**, 1-19 (1981).
- (11) H. Gruler and E. Sackmann. Croat. Chem. Acta, **49**, 379-388 (1977).
- (12) G. D. Eytan and R. Broza. J. Biol. Chem., **253**, 3196-3202 (1978).
- (13) J. Braun, J. R. Abney and J. C. Owicki. Biophys. J., **45**, 147a (1984).
- (14) C. R. Hartzell and H. Reinert. Biochim. Biophys. Acta, **368**, 317-338 (1974).
- (15) D. M. Rice, J. C. Houg, T. E. King and E. Oldfield. Biochemistry, **18**, 5885-5892 (1979).
- (16) G. C. Ruben, J. N. Telford and R. C. Carroll. J. Cell Biol., **68**, 724-439 (1976).
- (17) J. F. Deatherage, R. Henderson and R. A. Capaldi. J. Mol. Biol., **158**, 487-499 (1982).

- (18) J. C. Owicki and H. M. McConnell. Proc. Natl., Acad. Sci., U.S.A., **76**, 4750-4754 (1979).
- (19) M. S. Swanson, A. T. Quintahilla and D. D. Thomas. J. Biol. Chem., **255**, 7494-7502 (1980).
- (20) S. Y. Kang, H. S. Gutowsky, J. C. Hsung, R. Jacobs, T. E. King, D. Rice and E. Oldfield. Biochemistry, **18**, 3257-3267 (1979).
- (21) M. R. Paddy, F. W. Dahlquist, J.H. Davis and M. Bloom. Biochemistry, **20**, 3152-3162 (1981).
- (22) P. Jost, O. H. Griffith, R. A. Capaldi and G. Vanderkooi. Proc. Natl. Acad. Sci., U.S.A., **70**, 480-484 (1973).
- (23) P. F. Knowles, A. Watts and D. Marsh. Biochemistry, **18**, 4480-4487 (1979).
- (24) C. Rigell and E. Freire. Biophys. J., **45**, 358a abstr. (1984).
- (25) C. H. Chen and D. G. Friar. Biophys. J., **45**, 358a abstr. (1984).
- (26) C. P. Fan and M. J. Stephen. Phys. Rev. Lett., **25**, 500-503 (1970).
- (27) P. G. deGennes. "The Physics of Liquid Crystals"; Oxford University Press: 1973, Chapter 3.
- (28) J. Nehring and A. Saupe. J. Chem. Soc., Faraday Trans. II, **68**, 1-15 (1972).

CHAPTER 6

Summary and Conclusions

We have studied in this thesis the pair distribution functions (PDF's) from a number of model (synthetic) and natural membranes. From the PDF's, the qualitative nature, and in some cases, quantitative details of the interaction energies between sets of freeze-fracture particles can be deduced. Our major assumption is that the protein molecules can be modeled as a two-dimensional fluid, and that their lateral organization in a membrane can be simulated using the equations that have been developed in the field of liquid state physics.¹ The mobility of proteins in membranes is well established²⁻⁵ and there is no reason to doubt the validity of our assumptions.

We have observed three general kinds of inter particle interaction. These are: i) random, ii) attractive and iii) repulsive. A random distribution was observed for particles of bacteriorhodopsin (BR) which were reconstituted into phosphatidyl choline (PC) membranes of hydrocarbon region thicknesses up to 1 nm less than the thickness of the hydrophobic surface of the protein.^{6,7} Non-random protein distributions were observed in rhodopsin (RH)/PC recombinants. In general the interaction was repulsive. In one case (RH/di 18:1 trans PC) the interaction was attractive. The attractive potential was manifested as partial aggregation of the protein molecules in the plane of the bilayer.

An attractive interaction was observed in Acholeplasma laidlawii membranes from micrographs obtained from James and Branton.⁸ The measured PDF's could be simulated using a potential energy function that was derived by assuming that the protein molecules in a membrane perturb some scalar order parameter of the membrane, and that this perturbation occurs at

some energy cost. Solution of the appropriate Euler Lagrange differential equation shows that under circumstances in which a scalar parameter only is involved, an attraction between particles must result.

Finally, a series of measurements of the PDF's of particles of cytochrome c oxidase in membranes of dimyristoyl PC, cardiolipin and dimyristoyl phosphatidyl glycerol were carried out. In every case a long-ranged repulsion between particles was observed. In order to explain such a repulsion, it is necessary to invoke a vector order parameter of the bilayer that is being perturbed by protein. The average value of the director indicating lipid molecule orientation appears to be the most appropriate parameter to invoke here.⁹

In the present chapter we seek to examine the results that have been obtained and establish patterns in these results and directions for future work. In Chapter 1 ways were described in which a lipid bilayer might have to deform in order to fit the surface of an intercalated protein molecule. For BR/PC recombinants, the case illustrated in figures 2 and 3 of Chapter 1 was analyzed for the picture in which the protein is a right circular cylinder and the bilayer is thinner than protein. The BR monomer is known to consist of seven α -helices oriented approximately perpendicular to the bilayer normal.¹⁰ The freeze-fracture particle is probably a trimer and the effect on the lipid that is expected is an increase in the number of gauche conformers per lipid chain in order that the bilayer be thickened. Our results suggest that $E_{\text{def}} = 0$ in this case. This may come about either because the change in lipid conformation is not propagated to any great extent beyond the protein-lipid boundary or the energy cost of the conformational change

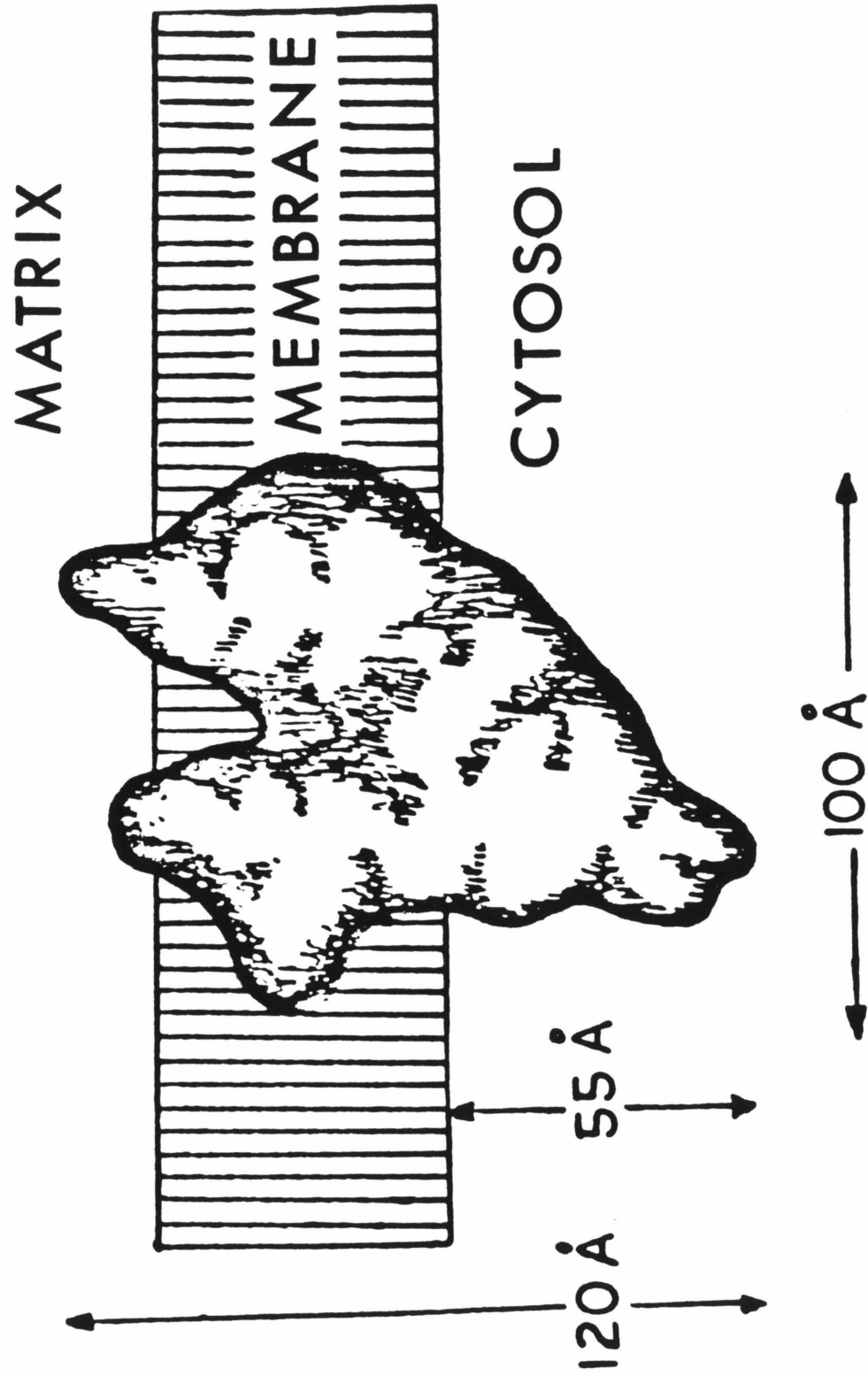
($k_1(\bar{\phi} - \phi_0)^2$ in equation 7, Chapter 4) is small. Studies of the charge in energy, ΔE , for a C-C bond to go from a trans to gauche conformation indicate that E is around one kT .¹⁷ The magnitude of $k_1(\bar{\phi} - \phi_0)^2$ should therefore be significant with respect to thermal energy and we are led to the conclusion that the correlation length is small for this type of charge in the bilayer.

Cytochrome c oxidase shows a very different kind of interaction when reconstituted in lipid bilayers. In all lipids, there are regions of membrane which contain patches of particles, but these particles repel each other. In figure 1 is shown a representation of the shape of the cytochrome c oxidase molecule.¹¹ The requirement that lipid pack around the protein means that a more severe perturbation of the bilayer will be necessary than for BR. In particular, tilting of entire lipid molecules appears to be necessary for lipid to accommodate the non-perpendicular protein surface.

Tilting of the lipid molecules has consequences for inter-protein interactions that have been pointed out by Gruler and Sackman.¹² The repulsion that is seen between protein particles is consistent with a number of deductions:

- i) A scalar lipid order parameter, such as was used in Chapter 4 to model attractive interactions, is inadequate to describe the effect of protein on the lipid membrane. Change in lipid orientation is described by a vector order parameter.

Figure 1. Sketch of the cross section of the cytochrome c oxidase molecule in the mitochondrion.



- ii) The splay and/or twist elastic constants of the bilayer membrane have magnitudes of the order of those seen in nematic and smectic liquid crystals.¹³
- iii) E_{def} is of the order of a few kT , by analogy with the values of E_1 that were obtained in Chapter 4 for partially aggregated systems.
- iv) The range of the interaction is determined by the extent of tilting of the lipid molecules at the protein-lipid boundary, as this is what determines the spatial rate of change of tilt in the region between protein molecules and therefore determines $\text{div } \mathbf{n}$ and $\text{curl } \mathbf{n}$ (Chapter 5), when \mathbf{n} is the unit vector in the direction of the lipid molecular tilt.

This last point is illustrated by deGennes¹³ in his treatment of the static distortions that occur in a nematic liquid crystal when the walls bounding the nematic induce changes in orientation at their surfaces. The free-energy density of a liquid crystal can be expanded in a continuum model in terms that contain $\text{div } \mathbf{n}$ and $\text{curl } \mathbf{n}$, but not \mathbf{n} itself. This is in contrast to the expansion of equation 1 (Chapter 5) in which terms in $\nabla \phi$ and $(\bar{\phi} - \phi_0)$ both appear. As a result, there is no restoring force tending to keep \mathbf{n} perpendicular to the lipid bilayer and the correlation length (analogous to η^{-1} of Chapter 4) is infinite. Variation of \mathbf{n} over the membrane surface is therefore due only to boundary constraints applied by protein

molecules. A complete solution to the Euler Lagrange differential equation that is derived from equation 4, Chapter 5, using appropriate many particle boundary conditions, will yield more detailed information on the nature of forces induced between protein molecules as a result of lipid tilt changes. One further point that is worthy of note is that the repulsive interaction between cytochrome c oxidase particles was essentially independent of the lipid used. Head group charge and lipid molecule cross-sectional area appeared to have no effect on the order of magnitude of the interaction that was seen.

The existence of patches of oxidase is a result of an attractive interaction between protein molecules and such an interaction may be a result of perturbation of a scalar order parameter by protein. We have proposed in Chapter 5 that, again by analogy with liquid crystal behavior, the parameter S (equation 3, Chapter 5) be used. If this is the case, then an effect on S by the protein seems to be correlated with the need for lipid molecules to tilt on a timescale that allows protein to reorganize as a result of tilt changes. BR in relatively thin membranes exhibits no aggregation behavior and no tilting of lipid molecules is expected for lipid to be able to fit protein. In thicker bilayers, partial aggregation of BR is seen.⁶ No PDF's were measured from the partially aggregated BR/PC systems, but accommodation of the protein by the bilayers might be expected to involve a change in orientation of the lipid for membrane thicker than protein.

The RH/PC recombinants displayed a mixture of the repulsive and attractive behavior depending on the lipid used and the state of the protein. It is difficult to analyze the data on these micrographs in the same terms as

have been used up to now, partly because of the lack of detailed knowledge of the shape of the protein. What is of interest, though, is the possibility of a physiological function for membrane lipids as a result of E_{def} changing as RH goes from the bleached state to the dark adapted state. E_{def} then becomes a part of the energy of a change in conformation of a protein molecule. Protein-protein interactions also change with change in protein state, and these interactions will determine to a large extent the selectivity of interaction between membrane bound components.

Our most important conclusion is that protein shape is a major determinant of the aggregation state of proteins in membranes, with all that that implies for membrane structure and function. Lipids can mediate the interactions between protein molecules and in some cases the lipid composition of a biological membrane may be varied to facilitate, or otherwise, the functioning of membrane bound component.

It is appropriate to examine at this point the relationship between lipid mediated effects on protein order and the nature of lipid order that is being examined when lipids are studied spectroscopically. Recent nuclear magnetic resonance (NMR) studies of lipid bilayers show how to isolate the slow component of the motions of multilayer dispersion¹⁴ and indicate that protein molecules modulate the amplitude of these slower cooperative lipid motions.¹⁵ The deuterium T_2 can be extracted from the lineshape of the spectrum of a deuterated bilayer using a suitable pulse sequence.¹⁴ The value of T_2 is sensitive to S , the nematic order parameter defined in Chapter 5, and a direct method therefore presents itself for evaluating both the effect of protein on long-ranged cooperative lipid order, and for correlating

this with protein distribution functions.

It would be appropriate also to reexamine the electron paramagnetic resonance (EPR) spectra of spin labeled lipids in the presence of protein molecules. Freed and coworker¹⁶ have shown that slow motions of spins produce EPR spectra that resemble the spectra obtained from lipid spin labels in the presence of protein. The conventional approach to analyzing lipid spin label spectra is to attempt a deconvolution into two components, one due to bulk lipid and one due to boundary lipid. This approach may simply be incorrect.

Raman spectroscopy has been used to study the parameter S in liquid crystals.¹⁸ Phospholipid dispersions have been studied by Raman spectroscopy.^{19,20} It seems likely that a synthesis of these two kinds of studies will yield information on the way that protein molecules affect lipid bilayers, and specifically the order parameter that is due to intermolecular cooperative motions.

References and Notes

- (1) F. Lado. J. Chem. Phys., **49**, 3092-3096 (1968).
- (2) R. Peters and R. J. Cherry. Proc. Natl. Acad. Sci., U.S.A., **79**, 4317-4321 (1982).
- (3) J. Yguerabide, J. A. Schmidt and E. E. Yguerabide. Biophys. J., **39**, 69-75 (1982).
- (4) M Edidin, Y. Zagayansky and T. J. Lardner. Science (Wash., D.C.), **191**, 466-468 (1976).
- (5) R. J. Peters, K. Peters, K. H. Tews and W. Bahr. Biochim. Biophys. Acta, **367**, 282-294 (1974).
- (6) B. A. Lewis and D. M. Engelman. J. Mol. Biol., **166**, 203-210 (1983).
- (7) B. A. Lewis and D. M. Engelman. J. Mol. Biol., **166**, 211-217 (1983).
- (8) R. James and D. Branton. Biochim. Biophys. Acta, **323**, 378-390 (1973).
- (9) J. Nehring and A. Saupe. J. Chem. Soc., Faraday, Trans. II, **68**, 1-15 (1972).
- (10) D. M. Engelman, R. Henerson, A. D. McLaughlin and B. A. Wallace. Proc. Natl. Acad. Sci., U.S.A., **77**, 2023-2077 (1980).
- (11) J. F. Deatherage, R. Henderson and R. A. Capaldi. J. Mol. Biol., **158**, 478-499 (1982).
- (12) H. Gruler and E. Sackman. Croat. Chim. Acta, **49**, 379-388 (1977).
- (13) P. G. deGennes. "The Physics of Liquid Crystals"; Oxford University Press: Oxford, 1973, Chapter 3.
- (14) L. Muller and S. I. Chan. J. Chem. Phys., **78**, 4341-4348 (1983).
- (15) B. A. Cornell, J. B. Davenport and F. Separovic. Biochim. Biophys.

Acta, **689**, 337-345 (1982).

- (16) E. Meirovitch and J. H. Freed. J. Phys. Chem., **84**, 3281-3294 (1980).
- (17) J. R. Scherer and R. G. Snyder. J. Chem. Phys., **72**, 5798-6808 (1980).
- (18) E. B. Priestley and P. S. Pershan. Mol. Cryst. Liq. Cryst., **23**, 369-373 (1973).
- (19) P. Yager and W. L. Peticolas. Biophys. J., **31**, 359-370 (1980).
- (20) R. Bansil, J. Day, M. Meadows, D. Rice and E. Oldfield. Biochemistry, **19**, 1938-1943 (1980).